In planta chromatin immunoprecipitation in *Zymoseptoria tritici* reveals chromatin-based regulation of putative effector gene expression

Jessica L. Soyer[1,2*], Jonathan Grandaubert[2,3], Janine Haueisen[2], Klaas Schotanus[2,4], Eva H. Stukenbrock[2]

[1]UMR BIOGER, INRA, AgroParisTech, Paris-Saclay University, 78850 Thiverval-Grignon, France

[2]Max Planck Institute for Evolutionary Biology, August-Thienemann-Str. 2, 24306 Plön, and Christian-Albrechts University of Kiel, Am Botanischen Garten 1-9, 24118 Kiel, Germany

[3]Present address: Department of Mycology, Fungal Biology and Pathogenicity Unit, Institut Pasteur, INRA, 75015, Paris, France

[4]Departments of Molecular Genetics and Microbiology (MGM), Pharmacology and Cancer Biology, and Medicine, Duke University Medical Center, Durham, North Carolina, United States of America

Short title: Histone dynamics in *Z. tritici* during infection

Keywords: Heterochromatin; effectors; gene regulation; ChIP; *Zymoseptoria tritici; Triticum aestivum*

Corresponding author: Jessica L. Soyer, jessica.soyer@inra.fr

Summary: 229; Introduction: 645; Results: 3101; Discussion: 1300; Experimental Procedures: 1097; Acknowledgements: 41; Figure & Table legends: 923.

Summary

During infection, pathogens secrete effectors, key elements of pathogenesis. In several phytopathogenic fungi, synchronous waves of effector genes are expressed during plant infection to manipulate and silence plant defenses. In *Zymoseptoria tritici*, causing septoria leaf blotch of wheat, at least two waves of effector genes are expressed, during the asymptomatic phase and at the switch to necrotrophy. The underlying factors responsible for the fine-tuned regulation of effector gene expression in this pathogen are unknown. Previously, a detailed map of the chromatin structure *in vitro* of *Z. tritici* was generated by chromatin immunoprecipitation followed by high-throughput sequencing (ChIP-seq) targeting histone modifications typical for euchromatin (di-methylation of the lysine 4 of the histone H3, H3K4me2) or heterochromatin (tri-methylation of the lysine 9 and 27 of the histone H3, H3K9me3 and H3K27me3). Based on the hypothesis that changes in the histone modifications contribute to the transcriptional control of pathogenicity-related genes, we tested whether different sets of genes are associated with different histone modifications *in vitro.* We correlated the *in vitro* histone maps with *in planta* transcriptome data and show that genes located in heterochromatic domains *in vitro* are highly up-regulated at the switch toward necrotrophy. We combined our integrated analyses of genomic, transcriptomic and epigenomic data with ChIP-qPCR *in planta* and thereby provide further evidence for the involvement of histone modifications in the transcriptional dynamic of putative pathogenicity-related genes of *Z. tritici*.

Introduction

Fungi that colonize plant tissues, pathogens as well as mutualists, express effector genes required for their establishment within the plant tissue (Lo Presti *et al*., 2015; Tyler and Rouxel, 2013). Transcriptomic analyzes have shown that effector genes are poorly expressed during axenic growth and strongly induced during host infection with several waves of concerted expression associated to infection stages (e.g. in *Melampsora larici-populina*, *Colletotrichum* species, *Leptosphaeria maculans*; Gervais *et al*., 2017; Hacquard *et al*., 2012; Lorrain *et al*., 2018; O'Connell *et al*., 2012). The fine-tuned regulation of effector genes is important for successful plant infection by fungi. However, very little is known about the underlying mechanisms that regulate expression of effector genes during different stages of host infection.

Transposable element (TE) rich regions of the genome are often enriched in genes encoding proteinaceous effectors or secondary metabolites (Soyer *et al*., 2015a). In the oilseed rape pathogen *L. maculans*, effector genes expressed during infection of young leaves are enriched in TE-rich regions while effector genes expressed during stem infection are enriched in gene-rich regions of the genome (Gervais *et al*., 2017).

In *L. maculans* and in the distantly related fungi *Epichloe festucae*, a symbiont of the grass *Lolium perenne*, it has been shown that histone modifications play a crucial role in the regulation of genes located in TE-rich regions involved in the establishment of fungus-plant interactions (Chujo and Scott 2014; Soyer *et al*., 2014). These studies support the hypothesis that chromatin-mediated gene regulation represents an efficient strategy to

63 control genes located in the vicinity of TEs.

64 *Zymoseptoria tritici* causes the septoria tritici blotch disease on wheat (*Triticum aestivum*)
65 (O'Driscoll *et al*., 2014). Infection conferred by *Z. tritici* is initiated by a asymptomatic
66 phase during which the pathogen grows intercellularly. Ten to 12 days post infection, the
67 fungus switches to a necrotrophic stage inducing host cell death. The release of nutrients
68 from dead plant cells allows the formation of pycnidia and the production of asexual
69 spores responsible for new infections. Thus, successful infection of *Z. tritici* involves a
70 lifestyle transition conferred by distinct transcriptional programs (Haueisen *et al*., 2018;
71 Rudd *et al*., 2015; Palma-Guerrero *et al.,* 2016). So far, little is known about the regulation
72 of the different infection programs set up by this fungus.
73
74 The genome of *Z. tritici* comprises 13 core chromosomes and a variable number of
75 accessory chromosomes showing presence-absence polymorphisms in different isolates
76 (Wittenberg *et al*., 2009; Goodwin *et al*., 2011; Möller *et al*., 2018). TEs represent 18% of
77 the genome with a considerably higher abundance on the accessory chromosomes than
78 on core chromosomes (Dhillon *et al*., 2014; Grandaubert *et al*., 2015). Transcriptomic
79 analyses revealed a dramatic difference in the expression of genes located on core and
80 accessory chromosomes, with the latter showing no or very low expression of most genes
81 *in vitro* as well as *in planta* (Kellner *et al*., 2014; Haueisen *et al*., 2018).
82 In a previous study, we performed chromatin immunoprecipitation followed by high-
83 throughput sequencing (ChIP-seq) *in vitro* to determine the genome-wide location of
84 histone modifications typical for euchromatin (di-methylation of the lysine 4 of the

histone H3, H3K4me2) or with heterochromatin (tri-methylation of the lysines 9 and 27 of H3, H3K9me3 and H3K27me3) (Schotanus *et al*., 2015). In *Z. tritici*, TE-rich regions are enriched with both heterochromatic marks, H3K9me3 and H3K27me3. Furthermore, we confirmed that transcriptional silencing of genes on the accessory chromosomes is due to the strong enrichment with heterochromatic DNA as these chromosomes are almost entirely associated with H3K27me3 (Schotanus *et al*., 2015).

Here, we investigated whether a chromatin-based control plays a role in the transcriptional regulation of pathogenicity-related genes in *Z. tritici*. We combined and integrated genomic, transcriptomic and epigenomic data and performed ChIP followed by quantitative PCR (ChIP-qPCR) analysis of targeted genes during plant infection. We provide evidence for an involvement of H3K9/K27me3 dynamics in the transcriptional regulation of putative pathogenicity genes of *Z. tritici*.

Results

Distribution of histone modifications in the coding fraction of the *Zymoseptoria tritici* genome

The ChIP-seq datasets generated from axenic cultures of the isolate Zt09 were analyzed to identify the genes associated with H3K4me2, H3K9me3 or H3K27me3. As previously described, H3K4me2 is mainly associated with gene-rich regions while the heterochromatin mark H3K9me3 is associated with the repetitive regions of the *Z. tritici* genome; H3K27me3 is likewise associated with repetitive sequences, telomeric regions,

accessory chromosomes, and with some gene coding sequences on core chromosomes.

We used the genome wide maps of H3K4me2, H3K9me3 and H3K27me3 from *in vitro* growth to distinguish genes either entirely or partially (> 1 bp) associated with each of the three histone modifications. Forty-two percent of the predicted genes in the genome are either associated with H3K4me2 (4,992 out of the 11,754 genes predicted in the genome), 0.75% (89 genes) with H3K9me3, 18.5% (2,179 genes) with H3K27me3 and 1.95% (230 genes) with both H3K9me3 and H3K27me3 (Figure 1A and 1B).

Genes located in H3K9me3 and H3K27me3 domains are less conserved and encode proteins putatively involved in virulence

We assessed the correlation of chromatin marks with the distribution of specific-specific genes previously identified in *Z. tritici* (Grandaubert *et al*., 2015). Using comparative genomics of four *Zymoseptoria* species, i.e., *Z. tritici*, *Zymoseptoria pseudotritici, Zymoseptoria ardabiliae and Zymoseptoria brevis*, we previously identified 1,717 genes unique to *Z. tritici*. We found that these genes are significantly enriched in regions of the genome that are associated with H3K27me3 domains and overlapping H3K9me3/ H3K27me3 domains: in total 951 of the *Z. tritici* species-specific genes locate in heterochromatic domains (X^2 test, $P < 0.01$; Table 1; Table S1). The *Z. tritici* genome encodes 874 putative effector genes and, interestingly, the species-specific genes are enriched in genes encoding putative effectors (177 representing 10.3% of the orphan genes; X^2 test; $P < 2.2.10^{-6}$) of which 82 locate in H3K9me3 and / or H3K27me3 domains.

In the *Z. tritici* reference genome, 6,329 predicted genes could not be assigned to a protein function (i.e. no homology with proteins predicted in other organisms and/or no protein domain included in databases). Hereinafter, we refer to these as genes of "unknown function". We found a significant enrichment of genes of unknown function in the heterochromatic domains enriched with H3K27me3 or enriched with both H3K9me3 and H3K27me3 (X^2 test, $P < 0.01$; Table 1; Table S2). Contrarily, genes associated with H3K4me2 were deprived of genes of unknown function compared to the rest of the genome (X^2 test, $P < 0.01$; Table S2). Taken together, these data suggest that heterochromatic DNA associates with less conserved genes, including many predicted to be secreted and involved in host-pathogen interactions.

H3K9me3 and H3K27me3 are associated with genes encoding putative pathogenicity determinants

Specific types of proteins are often associated with pathogenicity in fungi (for example proteinaceous effectors and proteins involved in secondary metabolite syntheses; Tyler and Rouxel, 2013). In some species, such as Aspergilli, secondary metabolite-encoding genes were found to be enriched in subtelomeric regions of the genome or near TEs (Gacek and Strauss, 2012). Furthermore, a chromatin-based regulation of these genes by post-translational histone modifications was demonstrated for gene clusters encoding polyketide synthase-like (PKS) proteins and non-ribosomal peptide synthase (NRPS) gene clusters, e.g. in the endophyte *E. festucae* (Chujo and Scott, 2014).

We assessed whether PKS and NRPS encoding genes are associated with the two heterochromatin marks studied here. In total, 2,498 predicted genes (21% of all genes) locate in heterochromatic domains during *in vitro* growth of *Z. tritici*. Among these, we identified several genes involved in secondary metabolism and detoxification, i.e. with a predicted function such as cytochrome P450, polyketide synthase or Major Facilitator Superfamily (MFS) transporters. More precisely, 11 genes of the *Z. tritici* genome were annotated as PKS and nine as NRPS encoding genes (Ohm *et al*., 2012; Grandaubert *et al*., 2015). PKS/NRPS encoding genes are significantly enriched in H3K27me3 domains as identified during *in vitro* growth of the fungus (X^2 test, $P < 0.01$, Table 1; Table S1).

We next used a PFAM enrichment analysis (Finn *et al*., 2014) to assess if genes encoding proteins involved in biosynthetic activities were also enriched in heterochromatic domains of the *Z. tritici* genome. We found that H3K27me3 and H3K9me3 domains are significantly enriched in genes involved in biosynthetic activities including genes encoding Rad51 PFAM domains known to be involved in DNA repair processes and genes encoding reverse transcriptases and transposases. Furthermore, genes located in H3K27me3 domains are enriched in PFAM protein families involved in secondary metabolism (Tables S3-6; FDR < 0.01).

We also analyzed the location of 227 genes predicted to encode Carbohydrate-Active Enzymes (CAZymes) in the *Z. tritici* genome. Contrary to secondary metabolite genes, there is no significant enrichment of the CAZyme genes in heterochromatic domains (X^2 test, $P > 0.01$; Table 1; Table S2).

In the pathogenic fungus *L. maculans*, effector genes showing stage-specific expression profiles during infection of oilseed rape (*Brassica napus*), are enriched in GC-poor or TE-rich genomic regions (Gervais *et al*., 2017). Interestingly, the silencing of genes located in TE-rich regions, *in vitro*, involves a chromatin-based control via H3K9me3 (Soyer *et al*., 2014). We addressed whether TE-rich genomic regions and heterochromatic domains of the *Z. tritici* genome likewise are enriched in putative effector genes. The 874 predicted effector genes represent eight percent of all predicted genes in *Z. tritici* and only nine on the accessory chromosomes (1.04% of all genes predicted on the accessory chromosomes). We here refined our analyses to address the association of the 865 putative effector genes of the core chromosomes and TEs. We considered a gene to be associated with TE regions if the gene locates within 2 kb distance of a TE. Assigning this criterion, we confirm that TE-rich regions of core chromosomes are enriched in putative effector genes (185 putative effector genes corresponding to 12.6% of the TE associated genes; X^2 test, $P < 0.01$; Table 2; Table S7; Figure 2). We also found a significant enrichment of putative effector genes in heterochromatic domains associated with TEs or not (H3K9me3, H3K27me3 and H3K9me3/H3K27me3 overlapping domains; Table 2; Table S7) while euchromatic domains are deprived of putative effector genes (X^2 test, $P < 0.01$; Table S7). Altogether, our analysis suggests that genes encoding putative pathogenicity-determinants are non-randomly distributed in the genome of *Z. tritici* and in particular enriched in H3K27me3 and H3K9me3 domains *in vitro*.

190 *In vitro* heterochromatic domains are enriched with genes up-regulated upon plant
191 infection

192 As genes predicted as putative pathogenicity determinants (PKS, NRPS, effector genes)
193 appear not to be randomly located in the genome of *Z. tritici*, we hypothesize that
194 regulation of the expression of these genes involves a chromatin-based control as shown
195 for effectors in *L. maculans* (Soyer *et al*., 2014). We therefore assessed the correlation of
196 the genome-wide expression patterns in the *Z. tritici* isolate Zt09 with the distribution of
197 genome-wide map of H3K4me2, H3K9me3 and H3K27me3 histone modifications
198 observed during *in vitro* growth (Schotanus *et al*., 2015). To this end, we processed
199 transcriptomic data generated from axenic cultures and infected plant material from
200 previous studies (Kellner *et al.,* 2014, Haueisen *et al*., 2018).

201 During axenic growth, 9,412 genes are expressed with RPKM ≥ 2. Ninety-eight percent
202 (3,237) of the genes for which sequence is entirely associated with H3K4me2, 58% and
203 39% of genes (i.e. 18 and 737 genes) associated with H3K9me3 or H3K27me3 respectively
204 were expressed *in vitro* (RPKM ≥ 2). These patterns confirm that H3K4me2 is almost
205 systematically associated with transcriptional activity while H3K9me3 and H3K27me3
206 represent repressive histone modifications (Wilcoxon-test, $P < 0.05$; Figure 3).

207 We then compared the transcriptomic profiles of Zt09 genes during host infection and
208 assessed genome wide expression patterns at 4 and 13 days post inoculation (dpi), i.e.
209 during early asymptomatic host infection and at the transition to necrotrophic growth,
210 respectively. We analyzed 1) the number and distribution of genes silenced during *in vitro*

211 growth and induced during plant infection and 2) the number and distribution of genes
212 significantly up- or down- regulated *in planta* compared to axenic culture (Figure 4).

213 We first analyzed genes specifically induced at 4 or 13 dpi compared to axenic culture (i.e.
214 RPKM ≤ 2 for the axenic culture and RPKM ≥ 2 at 4 or 13 dpi). Using these criteria we
215 found 559 genes induced at 4 dpi, including 92 genes that locate in an *in vitro* H3K4me2
216 domain and 149 in an *in vitro* H3K27me3 domain (the H3K4me2 domains comprise a total
217 of 4,992 genes and H3K27me3 a total of 2,179 genes) (Table 1; Table S2). This pattern
218 shows that H3K27me3 domains are enriched in genes specifically expressed at 4 dpi
219 compared to axenic culture (X^2 test, $P < 0.01$; Table 1; Table S2). At 13 dpi, 886 genes, not
220 expressed *in vitro*, are induced (i.e. RPKM ≤ 2 for the axenic culture and RPKM ≥ 2 at 13
221 dpi), including 98 genes located in an *in vitro* H3K4me2 domain and 355 genes located in
222 an *in vitro* H3K27me3 domain. For this later stage of infection, as for 4 dpi, we also found
223 that genes specifically expressed at 13 dpi compared to axenic culture are enriched in
224 genes associated with *in vitro* H3K27me3 domains (X^2 test, $P < 0.01$; Table 1; Table S2).

225 We next analyzed genes up-regulated *in planta* compared to the axenic culture (log2 Fold
226 Change (RPKM) ≥ 1 and FDR ≤ 0.001). At 4 dpi, 784 genes were significantly up-regulated
227 compared to the axenic growth. These up-regulated genes are significantly enriched in
228 genes encoding effector candidates (114 putative effector genes of all up-regulated genes
229 at 4 dpi; X^2 test, $P < 0.01$; Table 2; Table S7). However, during early infection, up-regulated
230 genes are not significantly associated with any of the histone modifications investigated
231 here. At 4 dpi, there is no effect of the *in vitro* location in H3K4me2, H3K9me3 or

H3K27me3 on the up- or down-regulation of genes (Table 1; Table S2; Figure 4A). At 13 dpi, 1,773 genes were specifically up-regulated compared to 4 dpi, including 388 genes and 507 genes located respectively in a H3K4me2 and in a H3K27me3 domain *in vitro*. As for 4 dpi, up-regulated genes were significantly enriched in effector genes (309 putative effector genes; X^2 test, $P < 0.01$; Table 2, Table S7). At 13 dpi, transcription of the genes located in an *in vitro* heterochromatic domain is significantly different from genes located in an *in vitro* euchromatic domain (Wilcoxon test, $P < 2.2.10^{-16}$; Figure 4B). We observe that genes showing low, or no, expression *in vitro* and associated with a histone modification typical for heterochromatin in this growing condition are significantly higher expressed at the switch to necrotrophy than genes associated *in vitro* with euchromatin (Table 1; Table S2). Up-regulated effector genes were likewise enriched in genes located in the vicinity of TEs (i.e. distance ≤ 2 kb) and H3K27me3 *in vitro* (Table 2; Table S7). Taken together, these data show that although sets of putative effector genes were highly expressed both 4 dpi and 13 dpi, the histone modifications associated with the genes possibly influences their expression only at the switch to necrotrophy.

KMT1, *KMT6* or *KMT1/KMT6* deletions deregulate expression of pathogenicity-related genes

In *Z. tritici*, *kmt1*, *kmt6* and *kmt1/kmt6* mutants were generated and gene expression was analyzed, *in vitro*, using RNA-seq (Moeller *et al.*, 2018). We processed these data to address whether KMT1 and / or KMT6 may influence pathogenesis-related genes.

253 Among the 100 most up-regulated genes in respectively the *kmt1*, *kmt6* and *kmt1/kmt6*
254 mutants, 59, 36 and 32% are over-expressed at 13 dpi compared to axenic culture in the
255 WT strain suggesting that both histone methyltransferases are involved in regulation of
256 genes highly expressed in the WT strain upon infection. We analyzed whether certain
257 categories of genes were significantly enriched among the deregulated genes in the
258 mutant background (Table 3). *KMT1* deletion induces the reorganization of H3K27me3
259 modification with a relocation of this modification to H3K9me3 regions (Moeller *et al*.,
260 2018). Hence, genes located in H3K9me3 are not significantly induced because of
261 H3K9me3 loss as they may still be repressed by the H3K27me3 modification (Table 3).
262 However, consistently with the relocation of H3K27me3, genes located in a H3K27me3
263 domain in the WT are significantly induced in the *kmt1* mutant (Table 3). We identified
264 that deregulated genes in the *kmt1*, *kmt6* or *kmt1*/*kmt6* mutants were significantly
265 enriched in SP-genes (i.e. 220 putative effectors within the 2,110 deregulated genes) and
266 genes associated with TE sequences while no significant association of the CAZymes
267 encoding genes was observed (Table 3; X^2 test, $P < 0.01$). Particularly, the 972 genes up-
268 regulated in at least one of the mutants include 118 putative effector genes. Deletions of
269 *KMT1* and *KMT6* also significantly influenced expression of genes otherwise found to be
270 induced during infection in the WT strain (Table 3). Genes up-regulated at 4 dpi compared
271 to axenic culture, or 13 dpi compared to 4 dpi, in the WT strain are also significantly
272 enriched in the deregulated genes in the different mutants (231 out of the 784 genes up-
273 regulated at 4 dpi and 646 out of the 1,773 genes up-regulated at 13 dpi are deregulated
274 in the mutants).

We analyzed the expression of a few randomly selected genes based on their location in a heterochromatin domain *in vitro*, by RT-qPCR, in *kmt1*, *kmt6* and *kmt1*/*kmt6* deletion mutants. Some of these genes are putative effector genes or orphan genes and some are up-regulated in the WT at 13 dpi compared to early infection (4 dpi) in wheat (Table 4). One gene located in a H3K27me3 domain was not influenced by none of the deletion (gene ID Zt09_chr_3_00231) while all other genes had their expression up-regulated due to the deletion of at least *KMT1*, *KMT6* or both.

Up-regulation of effector candidate genes *in planta* is associated with changes in chromatin structure

The analysis of *in vitro* ChIP-seq data and *in planta* RNA-seq data indicates that chromatin modifications might contribute to the expression of pathogenicity related genes. *KMT1* and *KMT1/KMT6* deletions resulted in impaired *in vitro* growth and host colonization is consistently reduced compared to the WT while *KMT6* deletion only slightly reduced infection abilities. In all deletion backgrounds no large effect on gene expression was observed (Moeller *et al*., 2018). Analyses of gene expression in *KMT1* or *KMT6* mutants appear not to be the most appropriate approach to disentangle influence of histone modifications on the regulation of pathogenicity related genes. Therefore, we further investigated histone modification dynamics, *in planta*, in the WT strain. We investigated whether the up-regulation of putative effector genes at 13 dpi is associated with a difference in the histone methylation patterns between *in vitro* and *in planta* growth. We compared the histone methylation patterns in the genomic sequence of different genes

296 that are lowly expressed *in vitro* and up-regulated during the lifestyle switch *in planta*,
297 using ChIP-qPCR. The histone H4 encoding gene, constitutively expressed, and a
298 transposable element, constitutively silenced (the DNA transposon, DTH_element
299 5_ZTIPO323, located on chromosome 9;) were used as controls in the experiment.

300 The three selected genes (Zt09_chr_5_00271; Zt09_chr_6_00192; Zt09_chr_9_00038)
301 encode putative effectors among the 10 most expressed genes in *Z. tritici* at 13 dpi and
302 these are considerably less expressed *in vitro* compared to the histone H4 gene (Table
303 S8). The putative effector gene Zt09_chr_9_00038 encodes a hydrophobin-like protein
304 considered to be a “core” necrotrophic effector, i.e. conserved in different isolates of *Z.*
305 *tritici* (Haueisen *et al*., 2018). Using ChIP-qPCR, we confirm the *in vitro* association of the
306 five genes with H3K4me2, H3K9me3 or H3K27me3 ("% of input" method). Consistently,
307 the histone H4 encoding gene was associated with H3K4me2 while the TE sequence was
308 associated with H3K9me3 and H3K27me3 and the three putative effector genes were
309 located in heterochromatic domains (H3K9me3 or H3K27me3) *in vitro* (Figure 5; Table
310 S8).

311 For the *in planta* material, we confirmed the chromatin immunoprecipitation by a qPCR
312 targeting the wheat Actin gene (Genebank accession number KC775780.1, cultivar BR34)
313 at 13 dpi. We validated that there was no product for the wheat actin primers in the ChIP
314 samples generated from fungal axenic culture. The abundance of H3K4me2 for the wheat
315 actin gene was considerably higher compared to levels of H3K9me3 and H3K27me3
316 (Figure S1). In order to compare values obtained for the fungal genes *in vitro* and *in planta*,

we calculated enrichment values of the targeted genes relatively to the fungal histone H4 gene. We firstly confirmed that this method led to the same conclusion as the "% input" method (Figure 5 and Table S8). Furthermore, we checked the difference in terms of enrichment between the gene promoter and the coding sequence: we applied qPCR following ChIP targeting the upstream gene sequence and the coding region of the gene Zt09_chr_6_00192. The levels of H3K4me2, H3K9me3, H3K27me3 shows the same profile across the promoter and coding sequence, i.e. level of any histone modifications is similarly high or low for the upstream gene sequence or the coding region of the gene (Figure 6) between the promoter and the coding sequence of a gene.

At 13 dpi, the three targeted effector genes are highly expressed (Table S8) and the relative enrichment of H3K4me2 remained low compared to histone H4 gene (% of H3K4me2 enrichment for these genes compared to histone H4 < 0.2). On the contrary, the levels of H3K9me3 decreased (a relative 3-fold lower amount of H3K9me3) for the genes Zt09_chr_5_00271 and Zt09_chr_9_00038. For two genes located in H3K27me3 *in vitro* (Zt09_chr_9_00038 and Zt09_chr_6_00192), levels of H3K27me3 were 6-22 fold lower at 13 dpi compared to axenic culture. This suggests that the up-regulation of these genes at 13 dpi is associated with a remodeling of the underlying chromatin structure in their genomic sequence (Figure 6) and that the influence of the chromatin structure on effector gene expression is due to a decrease of the heterochromatin marks rather than an increase of the euchromatic mark investigated here.

We have assessed the levels of H3K4me2, H3K9me3 and H3K27me3 for the TE relatively

to the histone H4 gene: levels of H3K9me3 and H3K27me3 decreased compared to the levels *in vitro* but remained very high when compared to histone H4 and the three tested putative effector genes, which are up-regulated at this stage. Assessment of the chromatin state at the genomic loci of these genes confirms that constitutively expressed genes, such as the histone H4 gene, remain associated with the euchromatic modification H3K4me2 while the expression changes of the three effector genes tested are associated with changes of the associated histone modifications during wheat infection. This data provide evidence of an involvement of chromatin dynamics for the *in planta* regulation of secreted protein encoding genes putatively involved in pathogenicity.

Discussion

In some plant pathogenic fungi, including *Z. tritici*, the expression profiles of effector genes was shown to be highly dynamic during host infection. By correlating genomic coordinates of predicted effector genes to transcriptome and epigenome data, we here provide evidence for a role of a chromatin-based gene regulation during plant infection of *Z. tritici*. In particular, candidate effector genes up-regulated during the transition from asymptomatic to necrotrophic growth are significantly enriched in regions of the genome that are transcriptionally silenced by a heterochromatin structure of the DNA during axenic growth. In this study, we analyzed levels of different histone modifications typical for heterochromatin or euchromatin *in planta* by applying ChIP-qPCR targeting the genomic loci of three effector genes that are among the most up-regulated genes at 13

359 dpi. Our experimental work provides evidence that histone modifications H3K9me3 and
360 H3K27me3 play a role for the transcriptional regulation of putative effector genes in *Z.*
361 *tritici* during wheat infection. Our targeted analysis *in planta* thereby suggests that the
362 dynamic expression of effector genes can be associated with a dynamic of the
363 heterochromatin marks H3K9me3 and H3K27me3.

364

365 ***Genes located in a heterochromatin domain* in vitro *are enriched in putative virulence***
366 ***related genes***

367 In other species, such as *L. maculans*, *Fusarium oxysporum*, Aspergilli species, genes
368 located in regions that are TE-rich, subtelomeric, lineage-specific, are often enriched in
369 genes encoding putative effectors or genes involved in secondary metabolite production
370 (Rouxel *et al*., 2011; Grandaubert *et al*., 2014; Ma *et al*., 2010; Faino *et al*., 2016;
371 Vlaardingerbroek *et al*., 2016). We find here that TE-rich genomic compartments of *Z.*
372 *tritici* encode species-specific genes and genes encoding putative effector proteins. The
373 fact that TE-rich regions are enriched in species-specific genes was also shown at the
374 within species level (Plissonneau *et al*., 2016). Interestingly, while the *Z. tritici* reference
375 strains presents eight accessory chromosomes which contain twice as much TEs as the
376 core chromosomes, they are not enriched in putative secreted protein encoding genes as
377 only nine are located on the accessory chromosomes. Genes encoding other types of
378 pathogenicity related genes such as PKS and NRPS were also enriched in H3K27me3
379 domains of core chromosomes. Together, these data show that in *Z. tritici*, pathogenicity-

related genes and genes involved in host specificity are enriched in repeat-rich, heterochromatic regions on the core chromosomes.

Genes highly expressed at the lifestyle switch towards necrotrophy are enriched in genes located in heterochromatin* in vitro *and in effector candidates

Using our previous RNA-seq data generated *in vitro* and at 4 and 13 dpi (Kellner *et al*., 2014; Haueisen *et al*., 2018), we investigated patterns of gene expression as a function of their location in euchromatin or a heterochromatin domain *in vitro*. Genes over-expressed at 4 dpi compared to axenic culture and at 13 dpi compared to 4 dpi are enriched in putative pathogenicity-related genes. Interestingly, we found that genes highly expressed at the onset of the infection are not enriched in *in vitro* H3K4me2, H3K9me3 or H3K27me3 domains. However, genes highly expressed at the switch to necrotrophic growth are, *in vitro*, associated with TE sequences and H3K9me3 and H3K27me3. The different relevance of H3K9me3 and H3K27me3 at the two studied infection stages suggests that the pattern of histone modifications is dynamic during infection, and possibly influenced by signals from the host tissue and / or by fungal development *in planta*. It is possible that transcription of the genes highly expressed during the second wave of effector gene expression remains suppressed during early host infection to avoid induction of host immune responses. During early host infection, specific effectors are likely relevant to suppress the plant immune system upon host penetration and biotrophic fungal establishment.

401 Recently, functional analyses in *Z. tritici* have identified two genes encoding avirulence
402 proteins (i.e., effector that can be recognized by the immune system of the plant
403 activating defense reactions): Avr3D1 and AvrStb6, over-expressed during wheat
404 infection just before the switch to necrotrophic growth (Zhong *et al*., 2017; Meile *et al*.,
405 2018). In our ChIP-seq data, *AvrStb6,* located in a subtelomeric region, is associated with
406 H3K9me3 and H3K27me3 while *Avr3D1,* located close to repetitive sequences, is
407 associated with H3K27me3. Some of the genes encoding candidate necrosis inducing
408 proteins, highly expressed at the switch to necrotrophy, identified in a previous study
409 (Ben M'Barek *et al*., 2015) are also associated with heterochromatin domains *in vitro*, for
410 instance genes Zt09_chr_5_00190 or Zt09_chr_2_01243. The association of these genes
411 with H3K27me3 or TEs and their expression patterns support our findings drawn at the
412 genome wide scale.

413

414 ***The histone modification patterns is dynamic between* in vitro *and* in planta *stages for***
415 ***a few effector genes, influencing their expression***

416 The role of the chromatin structure for the regulation of effector genes in TE-rich regions
417 has been investigated in *L. maculans*, whereby RNAi-silenced transformants were
418 generated for genes encoding HP1 and KMT1, two players involved in heterochromatin
419 assembly and maintenance (Soyer *et al*., 2014). In this fungus, silencing of *HP1* and *KMT1*
420 led to an up-regulation of genes located in TE-rich regions, notably effector genes,
421 correlated with a decrease in H3K9me3 (Soyer *et al*., 2014). The same experimental

strategy was applied to investigate the role of histone modifications for the regulation of secondary metabolite-encoding genes in other fungal species including *F. graminearum*, *E. festucae* and Aspergilli species (Reyes-Dominguez *et al*., 2012; Chujo and Scott, 2014; Gacek-Matthews *et al*., 2015; Gacek-Matthews *et al*., 2016). In *E. festucae*, ChIP-qPCR was also applied *in planta* to analyze histone modification patterns at the genomic loci of secondary metabolite gene clusters located in subtelomeric areas. In *Fusarium fujikuroi*, deletion of the H3K36 methyltransferase or *KMT6* resulted in deregulation (either up- or down-regulation) of some secondary metabolite gene clusters (Janevska *et al*., 2018; Studt *et al*., 2016). These studies, together with other analyzing gene expression at the genome-wide scale in plant pathogenic fungi (Connolly *et al*., 2013; Soyer *et al*., 2014; Moeller *et al*., 2018) show that loss of histone methyltransferases result in derepression of some genes associated with the histone modifications while a fraction remains silenced suggesting that a very complex regulatory network is involved in their transcriptional control. As in Soyer *et al*. (2014), our analysis of gene expression in *KMT1*, *KMT6* mutants of *Z. tritici* (Moeller *et al*., 2018; our study) has shown that pathogenicity-related encoding genes and genes expressed upon infection, are enriched within the deregulated genes due to at least one of the deletion. In order to analyze influence of histone modifications in the WT context and during plant infection, we applied for the first time ChIP-qPCR *in planta* to analyze levels of H3K4me2, H3K9me3 and H3K27me3 of three genes encoding effector candidates which are highly expressed at 13 dpi, as well as the constitutively expressed histone H4 gene and a transposable element sequence. We could demonstrate that levels of H3K4me2, H3K9me3 and H3K27me3 for each targeted loci correlated with

444 their expression *in vitro* and at 13 dpi. For the repetitive element, levels of H3K9me3 and
445 H3K27me3 were high *in vitro* as well as *in planta* likely reflecting the efficient silencing of
446 TEs in some regions of the genome. However, effector genes associated with a high level
447 of H3K9me3 and H3K27me3 *in vitro* showed significantly reduced levels of these marks *in*
448 *planta* consistent with their strong up-regulation. This indicates that the chromatin
449 structure is dynamic between axenic culture and different infectious stages and
450 instrumental for regulation of gene expression, notably of at least some effector genes in
451 *Z. tritici*.

452 In conclusion, our study indicates a prominent role of chromatin-based gene regulation
453 during wheat infection of *Z. tritici*. The close association of putative effector genes with
454 repeat-rich DNA may facilitate rapid evolution of these genes. Furthermore, the
455 association with heterochromatin in these genomic compartments provides variability at
456 the transcriptional level possibly further facilitating the defeat of host defenses by this
457 important wheat pathogen.

458

459 **Experimental Procedures**

460 Fungal strain and plant cultivar

461 The *Z. tritici* isolate Zt09 was used throughout the study. Zt09 is derived from the
462 reference isolate IPO323, and differs by the absence of chromosome 18, lost during *in*
463 *vitro* culture (Kellner *et al*., 2014). Cultures were grown on solid yeast malt sucrose (YMS)

agar (4 g yeast extract, 4 g malt extract, 4 g sucrose, 20 g bacto agar, 1 liter H_2O) at 18°C in the dark. For the *in planta* experiments conducted in this study, *Triticum aestivum* cultivar Obelisk (Wiersum Plantbreeding, Winschoten, the Netherlands) was used. The *kmt1*, *kmt6* and *kmt1/kmt6* mutants were generated by Moeller *et al*. (2018).

Identification of genes associated with specific histone modifications

The annotation of the *Z. tritici* isolate presented in Grandaubert *et al*. (2015) was used in this study including genes predicted to encode putative effectors and Polyketide Synthases/NonRibosomal Peptide Synthetases. To distinguish genes associated with the different histone marks H3K4me2, H3K9me3 and H3K27me3, we used previously generated *in vitro* ChIP-seq datasets (Schotanus *et al*., 2015) available under the SRA accession number SRP059394. The Integrative Genome Viewer (IGV; http://www.broadinstitute.org/software/igv; Thorvaldsdóttir *et al.*, 2013) was used to visualize location of each domains along the genome. Statistically enriched regions were identified with RSEG (Song and Smith, 2011). We determined the *in vitro* chromatin state of each annotated gene using the previously published chromatin maps (Schotanus et *al*., 2015). Genes were considered to be associated with a given post-translational histone modification when partially (at least one bp) or completely located in a H3K4me2, H3K9me3 or H3K27me3 domain. A Chi^2 test was applied to identify statistical enrichment of euchromatic or heterochromatic domains for certain categories of genes: the expected proportion of a given category of genes across the entire genome was compared to the

485 observed distribution of the gene category in the H3K4me2, H3K9me3 or H3K27me3
486 domains. Enrichment was considered significant with a *P* value < 0.01. All analyses were
487 done in R (www.r-project.org).

488

489 RNA-sequencing datasets

490 To correlate gene expression with location in a given chromatin domain during *Z. tritici*
491 infection of wheat, we used previously generated *in vitro* and *in planta* (four and 13 dpi)
492 RNA-seq datasets of Zt09 (Kellner *et al*., 2014; Haueisen *et al*., 2018). RNA-seq data from
493 the *in vitro* grown cultures and the *in planta* stages are accessible at the NCBI Gene
494 Expression Omnibus respectively through accession number GSE54874 and GSE106136
495 (Kellner *et al*., 2014; Haueisen *et al*., 2018). RNA-seq data from the *kmt1*, *kmt6* and
496 *kmt1/kmt6* mutants during *in vitro* growth were generated by Moeller *et al*. (2018) and
497 at Sequence Read Archive under BioProject ID PRJNA494102.
498 RPKM values for each gene in a given condition were estimated using Cufflinks (Trapnell
499 *et al*., 2010) as already described in Kellner *et al*. (2014). The total read counts per
500 transcript were estimated in HTSeq using the intersection-strict mode (Anders *et al.,*
501 2015) and genes differentially expressed were identified with the EdgeR package
502 (Robinson *et al*., 2010) with a log2 Fold Change ≤ -1 or ≥ 1 and an associated false
503 discovery rate ≤ 0.001 (McCarthy *et al*., 2012). As previously conducted in a study of gene
504 expression in *Z. tritici* (Kellner *et al., 2*014), we only included genes with an RPKM value ≥
505 2 in the condition in which the gene is up-regulated.

506

507 Plant experiments for chromatin immunoprecipitation quantitative PCR analyses

508 Plant infections were done as previously described (Habig *et al*., 2017). In brief, the
509 second leaves of wheat seedlings were inoculated with a solution containing 1.10^7
510 cells/ml supplemented with 0.1% Tween by brushing an area of seven cm after 11 days of
511 seedling growth. Plant material was harvested four and 13 dpi for ChIP-qPCR. As a control,
512 non-inoculated leaves were also harvested four and 13 dpi.

513

514 Chromatin immunoprecipitation (ChIP) and quantitative PCR (qPCR)

515 ChIP with antibodies against H3K4me2, H3K9me3 and H3K27me3 was performed on cells
516 from axenic cultures as previously described (Soyer *et al.*, 2015). For *in planta* ChIP, 12
517 infected leaves were harvested (i.e. three leaves and four technical replicates) at 13 dpi
518 and the same protocol was used except that "native ChIP" (without formaldehyde
519 crosslinking) was applied from 100 mg of infected plant material. All DNA extractions were
520 done with the Wizard® SV Gel and PCR Clean Up system kit (Promega, Madison, USA).

521 Based on our analyses of transcriptome, genome and ChIP-seq data, we selected three
522 candidate genes for ChIP-qPCR analyses: Zt09_chr_5_00271, Zt09_chr_6_00192,
523 Zt09_chr_9_00038. These genes are lowly expressed *in vitro* and among the 10 most
524 expressed genes in *Z. tritici* 13 dpi of wheat. Moreover, they are associated with
525 heterochromatin during *in vitro* growth (Table S8; Schotanus *et al*., 2015). Furthermore,

we included the sequence of a transposable element (DTH_element5_ZTIPO323, located on chromosome 9, position 29,065-30,735) as well as the gene encoding histone H4 (ID Zt09_chr_6_00256) as controls for precipitation with anti-H3K9me3, anti-H3K27me3 antibodies and anti-H3K4me2 antibody, respectively.

Quantitative PCR (qPCR) was performed with SYBR Green PCR Master Mix (Applied Biosystem, Foster City, USA) on a 7900 Real Time PCR System (Applied Biosystems). Two biological replicates, and two technical replicates were processed. Primers were designed with the OligoPerfect Designer (ThermoFisher Scientific) to target amplification of products between 80 and 150 bp (Table S9). The efficiency of PCR primers was verified on genomic DNA as described previously (Taylor *et al*., 2010). For RT-qPCR, Ct values were analyzed as described in Muller *et al*. (2002) for analysis of expression profiles and the Glyceraldehyde-3-phosphate dehydrogenase (GAPDH)-encoding gene (ID Zt09_chr_2_00354) was used as a constitutively expressed reference gene, as in Poppe *et al.* (2015). A positive control for the *in planta* ChIP experiment was obtained by qPCR amplification of the wheat actin gene (Table S9). For qPCR after *in vitro* ChIP, the immunoprecipitated fraction of each gene was calculated by the "% of input" method (Lin *et al*., 2012). Following the qPCR experiment, the Ct values (number of cycles required for the fluorescent signal to cross the threshold) were retrieved from the 7900 SDS software. To compare enrichment of the histone modifications H3K4me2, H3K9me3, and H3K27me3 for each target gene *in vitro* and *in planta*, we compared Ct values of the target genes to Ct values of a reference gene, histone H4 (i.e., for example, ΔCtH3K4me2 = Ct gene H3K4me2 – Ct histone H4 H3K4me2). The same calculation was applied for the

548 histone H4 gene, therefore ΔCt = 1 for each modification for this gene. Finally, the
549 enrichment of each target gene with the three histone modifications was calculated as
550 described by Lin *et al*. (2012) using %H3K4me2 = $100/2^{\Delta Ct}$. This enrichment was compared
551 for each gene *in vitro* and *in planta* (at 13 dpi).

552

553 **Acknowledgments**

554 The authors thank members from the "Environmental Genomics" group, in particular
555 Mareike Moeller, and J.Y. Dutheil, for fruitful discussion. J.L. Soyer was funded by a Young
556 Scientist Funding by INRA. The study was supported by a Max Planck fellowship to EHS.

557

558 **Author contributions**

559 Conceived and designed the experiments: JLS, JG, EHS. Acquisition, analysis or
560 interpretation of the data: JLS, JG, JH, KS, EHS. Writing of the manuscript: JLS, EHS.

561

562 **References**

563 **Anders, S., Pyl, P.T. and Huber, W.** (2015) HTSeq--a Python framework to work with
564 high-throughput sequencing data. *Bioinformatics,* **31**, 166–169.

565 **Ben M'Barek, S., Cordewener, J.H., Tabib Ghaffary, S.M., van der Lee, T.A., Liu, Z.,**
566 **Mirzadi Gohari, A., Mehrabi, R., America, A.H., Robert, O., Friesen, T.L., Hamza, S.,**
567 **Stergiopoulos, I., de Wit, P.J. and Kema, G.H.** (2015) FPLC and liquid-chromatography

568 mass spectrometry identify candidate necrosis-inducing proteins from culture filtrates of
569 the fungal wheat pathogen *Zymoseptoria tritici*. *Fungal Genet. Biol.* **79**, 54–62.

570 **Chujo, T. and Scott, B.** (2014) Histone H3K9 and H3K27 methylation regulates fungal
571 alkaloid biosynthesis in a fungal endophyte-plant symbiosis. *Mol. Microbiol.*, **92**, 413–434.

572 **Connolly, L.R., Smith, K.M. and Freitag, M.** (2013) The *Fusarium graminearum*
573 histone H3K27 methyltransferase KMT6 regulates development and expression of
574 secondary metabolite gene clusters. *PLoS Genet.*, **9**, e1003916.

575 **Dhillon, B., Gill, N., Hamelin, R. and Goodwin, S.B.** (2014) The landscape of
576 transposable elements in the finished genome of the fungal wheat pathogen
577 *Mycosphaerella graminicola*. *BMC Genomics*, **15**, 1132.

578 **Faino, L., Seidl, M.F., Shi-Kunne, X., Pauper, M., van den Berg, G.C.M., Wittenberg,**
579 **A.H.J. and Thomma, B.P.** (2016) Transposons passively and actively contribute to
580 evolution of the two-speed genome of a fungal pathogen. *Genome Res.*, **26**, 1091–1100.

581 **Finn, R.D., Bateman, A., Clements, J., Coggill, P., Eberhardt, R.Y., Eddy, S.R., Heger,**
582 **A., Hetherington, K., Holm, L., Mistry, J., Sonnhammer, E.L., Tate, J. and Punta, M.** (2014)
583 Pfam: the protein families database. *Nucleic Acids Res.*, **42**, D222–230.

584 **Gacek, A. and Strauss, J.** (2012) The chromatin code of fungal secondary metabolite
585 gene clusters. *Appl. Microbiol. Biotechnol.*, **95**, 1389–1404.

586 **Gacek-Matthews, A., Noble, L.M., Gruber, C., Berger, H., Sulyok, M., Marcos, A.T.,**
587 **Strauss, J. and Andrianopoulos, A.** (2015) KdmA, a histone H3 demethylase with bipartite

588 function, differentially regulates primary and secondary metabolism in *Aspergillus*
589 *nidulans*. *Mol. Microbiol.*, **96**, 839–860.

590 **Gacek-Matthews, A., Berger, H., Sasaki, T., Wittstein, K., Gruber, C., Lewis, Z.A. and**
591 **Strauss, J.** (2016) KdmB, a Jumonji histone H3 demethylase, regulates genome-wide H3K4
592 trimethylation and is required for normal induction of secondary metabolism in
593 *Aspergillus nidulans*. *PLoS Genet.*, **12**, e1006222.

594 **Gervais, J., Plissonneau, C., Linglin, J., Meyer, M., Labadie, K., Cruaud, C., Fudal, I.,**
595 **Rouxel, T. and Balesdent, M.H.** (2017) Different waves of effector genes with contrasted
596 genomic location are expressed by *Leptosphaeria maculans* during cotyledon and stem
597 colonization of oilseed rape. *Mol. Plant Pathol.*, **18**, 1113–1126.

598 **Goodwin S.B., M'barek S.B., Dhillon B., Wittenberg A.H., Crane C.F., Hane J.K.,**
599 **Foster, A.J., Van der Lee, T.A., Grimwood, J., Aerts, A., Antoniw, J., Bailey, A., Bluhm, B.,**
600 **Bowler, J., Bristow, J., van der Burgt, A., Canto-Canché, B., Churchill, A.C., Conde-**
601 **Ferràez, L., Cools, H.J., Coutinho, P.M., Csukai, M., Dehal, P., De Wit, P., Donzelli, B., van**
602 **de Geest, H.C., van Ham, R.C., Hammond-Kosack, K.E., Henrissat, B., Kilian, A.,**
603 **Kobayashi, A.K., Koopmann, E., Kourmpetis, Y., Kuzniar, A., Lindquist, E., Lombard, V.,**
604 **Maliepaard, C., Martins, N., Mehrabi, R., Nap, J.P., Ponomarenko, A., Rudd, J.J.,**
605 **Salamov, A., Schmutz, J., Schouten, H.J., Shapiro, H., Stergiopoulos, I., Torriani, S.F., Tu,**
606 **H., de Vries, R.P., Waalwijk, C., Ware, S.B., Wiebenga, A., Zwiers, L.H., Oliver, R.P.,**
607 **Grigoriev, I.V. and Kema, G.H.** (2011) Finished genome of the fungal wheat pathogen
608 *Mycosphaerella graminicola* reveals dispensome structure, chromosome plasticity, and

609 stealth pathogenesis. *PLoS Genet.*, **7**, e1002070.

610 **Grandaubert, J., Lowe, R.G., Soyer, J.L., Schoch, C.L., Van de Wouw, A.P., Fudal I.,**
611 **Robbertse, B., Lapalu, N., Links, M.G., Ollivier, B., Linglin, J., Barbe, V., Mangenot, S.,**
612 **Cruaud, C., Borhan, H., Howlett, B.J., Balesdent, M.H. and Rouxel T.** (2014) Transposable
613 element-assisted evolution and adaptation to host plant within the *Leptosphaeria*
614 *maculans-Leptosphaeria biglobosa* species complex of fungal pathogens. *BMC Genomics*,
615 **15**, 891.

616 **Grandaubert, J., Bhattacharyya, A. and Stukenbrock, E.H.** (2015) RNA-seq-based
617 gene annotation and comparative genomics of four fungal grass pathogens in the genus
618 *Zymoseptoria* identify novel orphan genes and species-specific invasions of transposable
619 elements. *G3 (Bethesda)*, **5**, 1323–1333.

620 **Habig, M., Quade, J. and Stukenbrock, E.H.** (2017) Forward genetics approach
621 reveals host genotype-dependent importance of accessory chromosomes in the fungal
622 wheat pathogen *Zymoseptoria tritici. MBio*, **8**, 6.

623 **Hacquard, S., Joly, D.L., Lin, Y.C., Tisserant, E., Feau, N., Delaruelle, C., Legué, V.,**
624 **Kohler, A., Tanguay, P., Petre, B., Frey, P., Van de Peer, Y., Rouzé, P., Martin, F., Hamelin,**
625 **R.C. and Duplessis, S.** (2012) A comprehensive analysis of genes encoding small secreted
626 proteins identifies candidate effectors in *Melampsora larici-populina* (poplar leaf rust).
627 *Mol. Plant Microbe Interact.*, **25**, 279–293.

628 **Haueisen, J., Moeller, M., Eschenbrenner, C.J., Grandaubert, J., Seybold, H.,**

Adamiak, H. and Stukenbrock, E.H. (2018) Highly flexible infection programs in a specialized wheat pathogen. *Ecol. Evol.*, **9,** 275-294.

Jamieson, K., Rountree, M.R., Lewis, Z.A., Stajich, J.E. and Selker, E.U. (2013) Regional control of histone H3 lysine 27 methylation in *Neurospora*. *Proc. Natl. Acad. Sci. U S A.*, **110**, 6027–6032.

Janevska, S., Baumann, L., Sieber, C.M.K., Münsterkötter M., Ulrich, J., Kämper, J., Güldener, U. and Tudzynski, B. (2018) Elucidation of the two H3K36me3 histone methyltransferases Set2 and Ash1 in *Fusarium fujikuroi* unravels their different chromosomal targets and a major impact of Ash1 on genome stability. *Genetics*., **208**, 153–171.

Kellner, R., Bhattacharyya, A., Poppe, S., Hsu, T.Y., Brem, R.B. and Stukenbrock, E.H. (2014) Expression profiling of the wheat pathogen *Zymoseptoria tritici* reveals genomic patterns of transcription and host-specific regulatory programs. *Genome Biol. Evol*., **6**, 1353–1365.

Lin, X., Tirichine, L. and Bowler, C. (2012) Protocol: Chromatin immunoprecipitation (ChIP) methodology to investigate histone modifications in two model diatom species. *Plant Methods*, **8**, 48.

Lo Presti, L., Lanver, D., Schweizer, G., Tanaka, S., Liang, L., Tollot, M., Zuccaro, A., Reissmann, S. and Kahmann, R. (2015) Fungal effectors and plant susceptibility. *Annu. Rev. Plant Biol.*, **66**, 513–545.

649 **Lorrain, C., Marchal, C., Hacquard, S., Delaruelle, C., Pétrowski, J., Petre, B., Hecker,**
650 **A., Frey, P. and Duplessis, S.** (2018) The rust fungus *Melampsora larici-populina* expresses
651 a conserved genetic program and distinct sets of secreted protein genes during infection
652 of its two host plants, larch and poplar. *Mol. Plant Microbe Interact.*, **31**, 695-706.

653 **Ma, L.J., van der Does, H.C., Borkovich, K.A., Coleman, J.J., Daboussi, M.J., Di Pietro**
654 **A., Dufresne, M., Freitag, M., Grabherr, M., Henrissat, B., Houterman, P.M., Kang, S.,**
655 **Shim, W.B., Woloshuk, C., Xie, X., Xu, J.R., Antoniw, J., Baker, S.E., Bluhm, B.H.,**
656 **Breakspear, A., Brown, D.W., Butchko, R.A., Chapman, S., Coulson, R., Coutinho, P.M.,**
657 **Danchin, E.G., Diener, A., Gale, L.R., Gardiner, D.M., Goff, S., Hammond-Kosack, K.E.,**
658 **Hilburn, K., Hua-Van, A., Jonkers, W., Kazan, K., Kodira, C.D., Koehrsen, M., Kumar, L.,**
659 **Lee, Y.H., Li, L., Manners, J.M., Miranda-Saavedra, D., Mukherjee., M, Park, G., Park, J.,**
660 **Park, S.Y., Proctor, R.H., Regev, A., Ruiz-Roldan, M.C., Sain, D., Sakthikumar, S., Sykes,**
661 **S., Schwartz, D.C., Turgeon, B.G., Wapinski, I., Yoder, O., Young, S., Zeng, Q., Zhou, S.,**
662 **Galagan, J., Cuomo, C.A., Kistler, H.C. and Rep, M.** (2010) Comparative genomics reveals
663 mobile pathogenicity chromosomes in *Fusarium*. *Nature*, **464**, 367–373.

664 **McCarthy, D.J., Chen, Y. and Smyth, G.K.** (2012) Differential expression analysis of
665 multifactor RNA-Seq experiments with respect to biological variation. *Nucleic Acids Res.*,
666 **40**, 4288–4297.

667 **Meile, L., Croll, D., Brunner, P.C., Plissonneau, C., Hartmann, F.E., McDonald, B.A.**
668 **and Sánchez-Vallet, A.** (2018) A fungal avirulence factor encoded in a highly plastic
669 genomic region triggers partial resistance to septoria tritici blotch. *New Phytol.*, **219**,

1048–1061.

Moeller, M., Habig, M., Freitag, M. and Stukenbrock, E.H. (2018) Extraordinary genome instability and widespread chromosome rearrangements during vegetative growth. *Genetics* **210**, 517-529.

Moeller, M., Schotanus, K., Soyer, J.L., Haueisen, J., Happ, K., Stralucke, M., Happel, P., Smith, K.M., Connolly, L.R., Freitag, M., and Stukenbrock E.H. (2018) Destabilization of chromosome structure by histone H3 lysine 27 methylation. *BioRxiv.org.*

Muller, P.Y., Janovjak, H., Miserez, A.R., and Dobbie, Z. (2002) Processing of gene expression data generated by quantitative real-time RT-PCR. *BioTechniques,* **32,** 1372–1379.

O'Connell, R.J., Thon, M.R., Hacquard, S., Amyotte, S.G., Kleemann, J., Torres, M.F., Damm, U., Buiate, E.A., Epstein, L., Alkan, N., Altmüller, J., Alvarado-Balderrama, L., Bauser, C.A., Becker, C., Birren, B.W., Chen, Z., Choi, J., Crouch, J.A., Duvick, J.P., Farman, M.A., Gan, P., Heiman, D., Henrissat, B., Howard, R.J., Kabbage, M., Koch, C., Kracher, B., Kubo, Y., Law, A.D., Lebrun, M.H., Lee, Y.H., Miyara, I., Moore, N., Neumann, U., Nordström, K., Panaccione, D.G., Panstruga, R., Place, M., Proctor, R.H., Prusky, D., Rech, G., Reinhardt, R., Rollins, J.A., Rounsley, S., Schardl, C.L., Schwartz, D.C., Shenoy, N., Shirasu, K., Sikhakolli, U.R., Stüber, K., Sukno, S.A., Sweigard, J.A., Takano, Y., Takahara, H., Trail, F., van der Does, H.C., Voll, L.M., Will, I., Young, S., Zeng, Q., Zhang, J., Zhou, S., Dickman, M.B., Schulze-Lefert, P., Ver Loren van Themaat, E., Ma, L.J. and Vaillancourt, L.J. (2012) Lifestyle transitions in plant pathogenic *Colletotrichum* fungi

691 deciphered by genome and transcriptome analyses. *Nat. Genet.*, **44**, 1060–1065.

692 **O'Driscoll, A., Kildea, S., Doohan, F., Spink, J. and Mullins, E.** (2014) The wheat-
693 Septoria conflict: a new front opening up? *Trends Plant Sci*., **19**, 602–610.

694 **Ohm, R.A., Feau, N., Henrissat, B., Schoch, C.L., Horwitz, B.A., Barry, K.W., Condon,**
695 **B.J., Copeland, A.C., Dhillon, B., Glaser, F., Hesse, C.N., Kosti, I., LaButti, K., Lindquist,**
696 **E.A., Lucas, S., Salamov, A.A., Bradshaw, R.E., Ciuffetti, L., Hamelin, R.C., Kema, G.H.,**
697 **Lawrence, C., Scott, J.A., Spatafora, J.W., Turgeon, B.G., de Wit, P.J., Zhong, S., Goodwin,**
698 **S.B. and Grigoriev, I.V.** (2012) Diverse lifestyles and strategies of plant pathogenesis
699 encoded in the genomes of eighteen Dothideomycetes fungi. *PLoS Pathog.*, **8**, e1003037.

700 **Palma-Guerrero, J., Torriani, S.F., Zala, M., Carter, D., Courbot, M., Rudd, J.J.,**
701 **McDonald, B.A. and Croll, D.** (2016) Comparative transcriptomic analyses of
702 *Zymoseptoria tritici* strains show complex lifestyle transitions and intraspecific variability
703 in transcription profiles. *Mol Plant Pathol*., **17**, 845–859.

704 **Plissonneau, C., Stürchler, A. and Croll, D.** (2016) The evolution of orphan regions in
705 genomes of a fungal pathogen of wheat. *MBio*, **7**(5).

706 **Poppe, S., Dorsheimer, L., Happel, P. and Stukenbrock, E.H.** (2015) Rapidly evolving
707 genes are key players in host specialization and virulence of the fungal wheat pathogen
708 *Zymoseptoria tritici* (*Mycosphaerella graminicola*). *PLoS Pathog*., **11**, e1005055.

709 **Robinson, M.D., McCarthy, D.J. and Smyth, G.K.** (2010) edgeR: a Bioconductor
710 package for differential expression analysis of digital gene expression data.

Bioinformatics, **26**, 139–140.

Reyes-Dominguez, Y., Boedi, S., Sulyok, M., Wiesenberger, G., Stoppacher, N., Krska, R. and Strauss, J. (2012) Heterochromatin influences the secondary metabolite profile in the plant pathogen *Fusarium graminearum*. *Fungal Genet. Biol.*, **49**, 39–47.

Rouxel, T., Grandaubert, J., Hane, J.K., Hoede, C., van de Wouw, A.P., Couloux, A., Dominguez, V., Anthouard, V., Bally, P., Bourras, S., Cozijnsen, A.J., Ciuffetti, L.M., Degrave, A., Dilmaghani, A., Duret, L., Fudal, I., Goodwin, S.B., Gout, L., Glaser, N., Linglin, J., Kema, G.H., Lapalu, N., Lawrence, C.B., May, K., Meyer, M., Ollivier, B., Poulain, J., Schoch, C.L., Simon, A., Spatafora, J.W., Stachowiak, A., Turgeon, B.G., Tyler, B.M., Vincent, D., Weissenbach, J., Amselem, J., Quesneville, H., Oliver, R.P., Wincker, P., Balesdent, M.H. and Howlett, B.J. (2011) Effector diversification within compartments of the *Leptosphaeria maculans* genome affected by Repeat-Induced Point mutations. *Nat. Commun.*, **2**, 202.

Rudd, J.J., Kanyuka, K., Hassani-Pak, K., Derbyshire, M., Andongabo, A., Devonshire, J., Lysenko, A., Saqi, M., Desai, N.M., Powers, S.J., Hooper, J., Ambroso, L., Bharti, A., Farmer, A., Hammond-Kosack, K.E., Dietrich, R.A. and Courbot, M. (2015) Transcriptome and metabolite profiling of the infection cycle of *Zymoseptoria tritici* on wheat reveals a biphasic interaction with plant immunity involving differential pathogen chromosomal contributions and a variation on the hemibiotrophic lifestyle definition. *Plant Physiol.*, **167**, 1158–1185.

Schotanus, K., Soyer, J.L., Connolly, L.R., Grandaubert, J., Happel, P., Smith, K.M.,

Freitag, M. and Stukenbrock, E.H. (2015) Histone modifications rather than the novel regional centromeres of *Zymoseptoria tritici* distinguish core and accessory chromosomes. *Epigenetics Chromatin*, **8**, 41.

Song, Q. and Smith, A.D. (2011) Identifying dispersed epigenomic domains from ChIP-Seq data. *Bioinformatics*, **27**, 870–871.

Soyer, J.L., El Ghalid, M., Glaser, N., Ollivier, B., Linglin, J., Grandaubert, J., Balesdent M.H., Connolly, L.R., Freitag, M., Rouxel, T. and Fudal, I. (2014) Epigenetic control of effector gene expression in the plant pathogenic fungus *Leptosphaeria maculans*. *PLoS Genet*., **10**, e1004227.

Soyer, J.L., Rouxel, T. and Fudal, I. (2015a) Chromatin-based control of effector gene expression in plant-associated fungi. *Currl Opin. Plant Biol.*, **26**, 51–56.

Soyer, J.L., Möller, M., Schotanus, K., Connolly, L.R., Galazka, J.M., Freitag, M. and Stukenbrock E.H. (2015b) Chromatin analyses of *Zymoseptoria tritici*: Methods for chromatin immunoprecipitation followed by high-throughput sequencing (ChIP-seq). *Fungal Genet. Biol.*, **79**, 63–70.

Studt, L., Rösler, S.M., Burkhardt, I., Arndt, B., Freitag, M., Humpf, H.U., Dickschat, J.S. and Tudzynski, B. (2016) Knock-down of the methyltransferase Kmt6 relieves H3K27me3 and results in induction of cryptic and otherwise silent secondary metabolite gene clusters in *Fusarium fujikuroi*. *Environ. Microbiol.,* **18**, 4037–4054.

Taylor, S., Wakem, M., Dijkman, G., Alsarraj, M. and Nguyen, M. (2010) A practical

752 approach to RT-qPCR-Publishing data that conform to the MIQE guidelines. *Methods*, **50**,
753 S1–5.

754 **Thorvaldsdóttir, H., Robinson, J.T. and Mesirov, J.P.** (2013) Integrative Genomics
755 Viewer (IGV): high-performance genomics data visualization and exploration. *Brief.*
756 *Bioinform.*, **14**, 178–192.

757 **Trapnell, C., Williams, B.A., Pertea, G., Mortazavi, A., Kwan, G., van Baren, M.J.,**
758 **Salzberg, S.L., Wold, B.J. and Pachter, L.** (2010) Transcript assembly and quantification by
759 RNA-Seq reveals unannotated transcripts and isoform switching during cell
760 differentiation. *Nat. Biotechnol.*, **28**, 511–515.

761 **Tyler, B.M. and Rouxel, T.** Effectors of fungi and oomycetes: their virulence and
762 avirulence functions, and translocation from pathogen to host cells. 2013, In Molecular
763 Plant Immunity. G. Sessa, Ed., Wiley Blackwell Press, Chap. 7, pp. 123–167.

764 **Vlaardingerbroek, I., Beerens, B., Schmidt, S.M., Cornelissen, B.J. and Rep, M.**
765 (2016) Dispensable chromosomes in *Fusarium oxysporum* f. sp. lycopersici. *Mol. Plant*
766 *Pathol.*, **17**, 1455–1466.

767 **Wittenberg, A.H., van der Lee, T.A., Ben M'barek, S., Ware, S.B., Goodwin, S.B.,**
768 **Kilian, A., Visser, R.G., Kema, G.H. and Schouten, H.J.** (2009) Meiosis drives extraordinary
769 genome plasticity in the haploid fungal plant pathogen *Mycosphaerella graminicola*. *PLoS*
770 *One*, **4**, e5863.

771 **Zhong, Z., Marcel, T.C., Hartmann, F.E., Ma X., Plissonneau, C., Zala, M., Ducasse,**

A., Confais, J., Compain, J., Lapalu, N., Amselem, J., McDonald, B.A., Croll, D. and Palma-Guerrero, J. (2017) A small secreted protein in *Zymoseptoria tritici* is responsible for avirulence on wheat cultivars carrying the Stb6 resistance gene. *New Phytol*., **214**, 619–631.

Figure legends

Figure 1. Euchromatic domains encompass more genes than heterochromatin domains *in vitro*. Venn diagrams showing genes associated with the different post-translational histone modifications assessed using ChIP-sequencing in axenic culture. A) Genes at least partially associated with any of the histone modification. B) Genes completely associated with any of the histone modifications.

Figure 2. Heterochromatic domains are enriched with putative effector genes that are up-regulated during the switch towards necrotrophic growth on wheat. Example from a section of chromosome 5, harboring the putative effector gene ID Zt09_chr_5_00271. Regions enriched in different histone modifications were identified using ChIP-seq with antibodies against H3K4me2 (light blue), H3K9me3 (purple), H3K27me3 (orange) and compared to the location of genomic features (coding sequences, dark blue; transposable elements, red) and to reads obtained by RNA-seq in axenic culture, 4 days post-infection (dpi) and 13 dpi.

Figure 3. Genes associated with euchromatin are expressed while genes associated with

792 **heterochromatin are repressed.** Expression assessed during axenic culture using RNA-
793 sequencing. Boxplot of the log_{10}(RPKM) of the genes totally associated with any of the
794 histone modification.

795 **Figure 4. Genes associated with euchromatin and heterochromatin *in vitro* exibit**
796 **different expression profiles *in planta*.** Boxplot of the log_{10} Fold Change (RPKM) of the
797 genes located in a euchromatic domain *in vitro* (i.e. H3K4me2) or a heterochromatic
798 domain *in vitro* (i.e. H3K9me3, H3K27me3 or H3K9me3/H3K27me3). Expression assessed
799 during axenic culture and at 4 and 13 days post infection (dpi) using RNA-sequencing;
800 genes differentially expressed at 4 dpi vs. axenic culture (A) or 13 dpi vs. 4 dpi (B). *:
801 Wilcoxon-test, $P < 2.2.10^{-16}$: comparison of heterochromatic-associated genes between 4
802 and 13 dpi.

803 **Figure 5. Putative effector genes are enriched in H3K9me3 and/or H3K27me3 *in vitro***
804 **while histone H4 is enriched in H3K4me2.** Chromatin immunoprecipitation was
805 performed during axenic culture to assess the levels of H3K4me2, H3K9me3 and
806 H3K27me3 in the genomic sequence of four genes (H4, Histone H4: Zt09_chr_6_00256;
807 5_00271: Zt09_chr_5_00271; 6_00192: Zt09_chr_6_00192; 9_00038:
808 Zt09_chr_9_00038) and a transposable element (DTH_element5_ZTIPO323).

809 **Figure 6. The up-regulation of three effector genes *in planta* is associated with a change**
810 **of their histone modifications patterns.** ChIP was performed at 13 days post infection of
811 wheat leaves by *Zymoseptoria tritici* and relative enrichment of (A) H3K4me2, (B)
812 H3K9me3 and (C) H3K27me3 was assessed using qPCR and compared during the axenic

813 culture and at 13 dpi. 5_00271: Zt09_chr_5_00271; 6_00192: Zt09_chr_6_00192;
814 6_00192 pro: Zt09_chr_6_00192, promoter; 9_00038: Zt09_chr_9_00038; K4, K9 and
815 K27: H3K4me2, H3K9me3 and H3K27me3 respectively. Blue: axenic culture; red: 13 dpi.

816

817 **Table legends**

818 **Table 1. Number of genes in a given category according to their location in a H3K4me2,**
819 **H3K9me3, H3K27me3 or H3K9me3/H3K27me3 domain *in vitro.***

820 [a]"unknown" genes are genes encoding predicted or hypothetical proteins;

821 [b]Genes located up to 2 kb upstream or downstream to a transposable element sequence;

822 [c]Genes specifically expressed at 4 or 13 days post infection (dpi) compared to axenic
823 culture or 4 dpi when RPKM ≥ 2 at the time point and RPKM ≤ 2 during the axenic culture
824 or at 4 dpi;

825 [d]Up-regulated genes are genes with Log2 Fold Change (RPKM) ≥ 1 and FDR ≤ 0.001 in a
826 given condition compared to the other;

827 [e]Down-regulated genes are genes with Log2 Fold Change (RPKM) ≤ -1 and FDR ≤ 0.001 in
828 a given condition compared to the other;

829 [f]Genes located in a H3K4me2, H3K9me3, H3K27me3 or H3K9me3/H3K27me3 domain *in*
830 *vitro*.

831

832 **Table 2. Number of putative effector genes located in vicinity to a transposable element**
833 **or in a H3K4me2, H3K9me3, H3K27me3 and H3K9me3/H3K27me3 domain *in vitro.***

834 Only putative effector genes located in the core genome of *Z. tritici* are shown here.

835 [a]Up-regulated genes are genes with Log2 Fold Change (RPKM) ≥ 1 and FDR ≤ 0.001 in a

836 given condition compared to the other;

837 [b]Down-regulated genes are genes with Log2 Fold Change (RPKM) ≤ -1 and FDR ≤ 0.001 in

838 a given condition compared to the other;

839 [c]Genes located up to 2 kb upstream or downstream to a transposable element sequence;

840 [d]Genes located in a H3K4me2, H3K9me3, H3K27me3 or H3K9me3/H3K27me3 *in vitro*.

841

842 **Table 3. Influence of *kmt1*, *kmt6* or *kmt1/kmt6* deletions on gene expression.**

843 [a]Genes located in a H3K4me2, H3K9me3, H3K27me3 or H3K9me3, H3K27me3 *in vitro*;

844 [b]"unknown" genes are genes encoding predicted or hypothetical proteins;

845 [c]Genes located up to 2 kb upstream or downstream to a transposable element sequence;

846 [d]Genes specifically expressed at 4 or 13 days post infection (dpi) compared to axenic

847 culture or 4 dpi when RPKM ≥ 2 at the time point and RPKM ≤ 2 during the axenic culture

848 or at 4 dpi;

849 [e]Up-regulated genes are genes with Log2 Fold Change (RPKM) ≥ 1 and FDR ≤ 0.001 in a

850 given condition compared to the other;

851 [g]Down-regulated genes are genes with Log2 Fold Change (RPKM) ≤ -1 and FDR ≤ 0.001 in

852 a given condition compared to the other;

853 [h]Genes deregulated in *KMT1*, *KMT6* or *KMT1/KMT6* deletions background, Log2 Fold

854 Change (RPKM) ≤ -1 or ≥ 1 and FDR ≤ 0.001.

855 Bold: the given domain contains significantly less genes of the given category compared

to the rest of the genome; grey: the given domain is enriched for the category of genes compared to the rest of the genome.

Table 4. Expression of selected genes associated with heterochromatin *in vitro*, in the *KMT1*, *KMT6* and *KMT1/KMT6* deletion mutants.

[a]Genes located up to 2 kb upstream or downstream to a transposable element sequence;

[b]Genes located in a H3K4me2, H3K9me3, H3K27me3 or H3K9me3, H3K27me3 *in vitro*;

[c]Genes significantly up-regulated 13 days post-infection (dpi) compared to 4 dpi;

[d]Gene expression relative to the WT strain and to the GAPDH encoding gene.

Supplementary data legends

Figure S1. Wheat actin was enriched in histone H3K4me2 and was used as a control for chromatin immunoprecipitation *in planta.* ChIP was performed at 13 days post infection of wheat leaves by *Zymoseptoria tritici*. Enrichment of the wheat actin gene in H3K4me2, H3K9me3 and H3K27me3 was assessed using qPCR.

Table S1. Enrichment analysis of PKS/NRPS- and orphan genes in a H3K4me2, H3K9me3, H3K27me3 or H3K9me3/H3K27me3 domain *in vitro.*

[a]Genes encoding PKS, NRPS, and orphan genes as predicted by Grandaubert *et al*. (2015);

[b]Genes with a RPKM ≥ 2;

[c]Genes with Log2 Fold Change (RPKM) ≥ 1 and FDR ≤ 0.001 at 4 days post infection (dpi)

878 compared to axenic culture or 13 dpi compared to 4 dpi were considered as up-regulated
879 at a given time point compared to the other. Only the genes with a RPKM ≥ 2 at least at
880 the time point during which it is up-regulated were kept for the analysis;
881 [d]Genes with Log2 Fold Change (RPKM) ≤ -1 and FDR ≤ 0.001 at 4 days post infection (dpi)
882 compared to axenic culture or 13 dpi compared to 4 dpi were considered as down-
883 regulated at a given time point compared to the other;
884 [e]Genes located in a H3K4me2, H3K9me3, H3K27me3 or H3K9me3/H3K27me3 *in vitro* as
885 identified with RSEG (see Experimental Procedures; Schotanus *et al*., 2015).
886 Blue: the given domain contains significantly less genes of the given category compared
887 to the rest of the genome; orange: the given domain is enriched for the category of genes
888 compared to the rest of the genome.
889
890 **Table S2. Enrichment analysis of genes of a given category in a H3K4me2, H3K9me3,**
891 **H3K27me3 or H3K9me3/H3K27me3 domain *in vitro.***
892 [a]Genes of "unknown function" are genes encoding predicted or hypothetical proteins;
893 genes encoding CAZymes as predicted by Grandaubert *et al*. (2015);
894 [b]Genes located up to 2 kb upstream or downstream to a transposable element sequence
895 as predicted by Grandaubert *et al*. (2015);
896 [c]Genes with a RPKM ≥ 2;
897 [d]Genes with Log2 Fold Change (RPKM) ≥ 1 and FDR ≤ 0.001 at 4 days post infection (dpi)
898 compared to axenic culture or 13 dpi compared to 4 dpi were considered as up-regulated
899 at a given time point compared to the other. Only the genes with a RPKM ≥ 2 at least at

the time point during which it is up-regulated were kept for the analysis;

[e]Genes with Log2 Fold Change (RPKM) ≤ -1 and FDR ≤ 0.001 at 4 dpi compared to axenic culture or 13 dpi compared to 4 dpi were considered as down-regulated at a given time point compared to the other;

[f]Genes located in a H3K4me2, H3K9me3, H3K27me3 or H3K9me3/H3K27me3 *in vitro* as identified with RSEG (see Experimental Procedures; Schotanus *et al*., 2015).

Blue: the given domain contains significantly less genes of the given category compared to the rest of the genome; orange: the given domain is enriched for the category of genes compared to the rest of the genome.

Table S3. PFAM analysis of the genes located in H3K4me2 domains *in vitro*.

Table S4. PFAM analysis of the genes located in H3K9me3/H3K27me3 domains *in vitro*.

Table S5. PFAM analysis of the genes located in H3K9me3 domains *in vitro*.

Table S6. PFAM analysis of the genes located in H3K27me3 domains *in vitro*.

Table S7. Enrichment analysis of putative effector genes in the vicinity of a transposable element or in a H3K4me2, H3K9me3, H3K27me3 and H3K9me3/H3K27me3 domain *in vitro*, and according to their expression.

[a]Genes encoding predicted secreted proteins (SP) were considered as genes encoding

putative effector genes for this study, as predicted by Grandaubert *et al*. (2015);

[b]Genes with Log2 Fold Change (RPKM) ≥ 1 and FDR ≤ 0.001 at 4 days post infection (dpi) compared to axenic culture or 13 dpi compared to 4 dpi were considered as up-regulated at a given time point compared to the other. Only the genes with a RPKM ≥ 2 at least at the time point during which it is up-regulated were kept for the analysis;

[c]Genes with Log2 Fold Change (RPKM) ≤ -1 and FDR ≤ 0.001 at 4 dpi compared to axenic culture or 13 dpi compared to 4 dpi were considered as down-regulated at a given time point compared to the other;

[d]Genes located up to 2 kb upstream or downstream to a transposable element sequence as predicted by Grandaubert *et al*. (2015);

[e]Genes located in a H3K4me2, H3K9me3, H3K27me3 or H3K9me3/H3K27me3 *in vitro* as identified with RSEG (see Experimental Procedures; Schotanus *et al*., 2015).

Blue: the given domain contains significantly less genes of the given category compared to the rest of the genome; orange: the given domain is enriched for the category of genes compared to the rest of the genome.

Table S8. Trimethylation of lysine 9 and / or 27 of histone H3 is reduced for three candidate effector genes up-regulated 13 days post infection of wheat leaves compared to axenic culture.

[a]Orphan genes as described by Grandaubert *et al*. (2015);

[b]Genes located at a distance below 2 Kb of a transposable element (Grandaubert *et al*., 2015);

[c]Relative enrichment*, in vitro* or 13 dpi, of H3K4me2, H3K9me3 or H3K27me3 for the given locus compared to histone H4 encoding gene (Zt09_chr_6_00256);

[d]Gene expression *in vitro* (Kellner *et al*., 2014);

[e]Gene expression from Haueisen *et al*. (2018);

[f]Expression rank of the candidate genes at 13 days post infection (dpi).

Table S9. List of primers used in this study.

Table 1. Number of genes in a given category according to their location in a H3K4me2, H3K9me3, H3K27me3 or H3K9me3/H3K27me3 domain *in vitro.*

	genome		H3K4me2-domains[f]		H3K9me3-domains[f]		H3K27me3-domains[f]		H3K9me3+H3K27me3-domains[f]	
	nb. in the entire genome	nb. in the core genome	nb. in the entire genome	nb. in the core genome	nb. in the entire genome	nb. in the core genome	nb. in the entire genome	nb. in the core genome	nb. in the entire genome	nb. in the core genome
total number of genes	11754	11111	4992	4991	89	89	2179	1661	230	171
unknown[a]	6329	5699	1944	1943	50	50	1734	1223	193	152
PKS/NRPS	20	20	1	1	0	0	10	10	0	0
CAZymes	227	227	58	58	4	4	32	32	3	3
genes < 2 Kb Tes[b]	1723	1464	369	368	83	83	545	358	202	154
orphan genes	1717	1221	177	177	21	21	794	392	136	91
genes expressed at 4 dpi vs axenic[c]	559	546	92	92	4	4	149	138	9	9
genes expressed at 13 dpi vs axenic[c]	886	778	98	98	10	10	355	253	20	17
genes expressed at 13 dpi vs 4 dpi[c]	729	577	53	53	10	10	368	224	27	20
genes up-regulated at 4 dpi vs. *in vitro*[d]	784	775	290	290	6	6	118	112	10	10
genes down-regulated at 4 dpi vs. *in vitro*[e]	1027	1001	379	379	3	3	179	156	23	21
genes up-regulated at 13 dpi vs. 4 dpi[d]	1773	1630	388	388	12	12	507	390	38	32
genes down-regulated at 13 dpi vs. 4 dpi[e]	798	796	385	385	5	5	81	80	12	11

[a]"unknown" genes are genes encoding predicted or hypothetical proteins;
[b]Genes located up to 2 kb upstream or downstream to a transposable element sequence;
[c]Genes specifically expressed at 4 or 13 days post infection (dpi) compared to axenic culture or 4 dpi when RPKM ≥ 2 at the time point and RPKM ≤ 2 during the axenic culture or at 4 dpi;
[d]Up-regulated genes are genes with Log2 Fold Change (RPKM) ≥ 1 and FDR ≤ 0.001 in a given condition compared to the other;
[e]Down-regulated genes are genes with Log2 Fold Change (RPKM) ≤ -1 and FDR ≤ 0.001 in a given condition compared to the other;
[f]Genes located in a H3K4me2, H3K9me3, H3K27me3 or H3K9me3/H3K27me3 domain *in vitro*.

Table 2. Number of putative effector genes located in vicinity to a transposable element or in a H3K4me2, H3K9me3, H3K27me3 and H3K9me3/H3K27me3 domain *in vitro*.

	core genome	TE-associated genes[c]	H3K4me2-domains[d]	H3K9me3-domains[d]	H3K27me3-domains[d]	H3K9+H3K27me3-domains[d]
total number of genes	11111	1464	4991	89	1661	171
putative effector genes	865	185	168	15	205	26
putative effector genes up-regulated at 4 dpi vs axenic[a]	114	14	24	3	22	1
putative effector genes down-regulated at 4 dpi vs axenic[b]	107	32	23	0	29	6
putative effector genes up-regulated at 13 dpi vs 4 dpi[a]	309	84	42	4	87	12
putative effector genes down-regulated at 13 dpi vs 4 dpi[b]	74	10	22	1	10	1

Only putative effector genes located in the core genome of *Z. tritici* are shown here.

[a]Up-regulated genes are genes with Log2 Fold Change (RPKM) ≥ 1 and FDR ≤ 0.001 in a given condition compared to the other;
[b]Down-regulated genes are genes with Log2 Fold Change (RPKM) ≤ -1 and FDR ≤ 0.001 in a given condition compared to the other;

[c]Genes located up to 2 kb upstream or downstream to a transposable element sequence;

[d]Genes located in a H3K4me2, H3K9me3, H3K27me3 or H3K9me3/H3K27me3 *in vitro*.

Table 3. Number of genes deregulated due to *KMT1*, *KMT6* or *KMT1/KMT6* deletions, *in vitro*.

	genome		*Δkmt1*[h]				*Δkmt6*[h]			
			up-regulated		down-regulated		up-regulated		down-regulated	
	nb. in the genome	proportion	nb. in the genome	proportion	nb. in the genome	proportion	nb. in the genome	proportion	nb. in the genome	proportion
total number of genes	11754		579		284		274		481	
H3K4me2[a]	4992	0.425	116	**0.200**	71	**0.250**	92	**0.336**	194	0.403
H3K9me3[a]	89	0.008	4	0.007	8	0.028	0		2	0.004
H3K27me3[a]	2179	0.185	168	0.290	57	0.201	116	0.423	63	**0.131**
H3K9/K27me3[a]	230	0.020	20	0.035	16	0.056	23	0.084	5	0.010
unknown[b]	6329	0.538	399	0.689	117	0.412	175	0.639	175	**0.364**
CAZymes	227	0.019	10	0.017	9	0.032	7	0.026	7	0.015
putative effectors	874	0.074	88	0.152	56	0.197	24	0.088	59	0.123
genes < 2 Kb Tes[c]	1723	0.147	112	0.193	83	0.292	79	0.288	64	0.133
orphan genes	1717	0.146	101	0.174	33	0.116	88	0.321	27	**0.056**
genes expressed at 4 dpi vs axenic[d]	559	0.048	55	0.095	0	NA	3	0.011	7	**0.015**
genes expressed at 13 dpi vs axenic[d]	886	0.075	121	0.209	2	0.007	25	0.091	9	**0.019**
genes expressed at 13 dpi vs 4 dpi[d]	729	0.062	105	0.181	12	0.042	44	0.161	21	0.044
genes up-regulated at 4 dpi vs. *in vitro*[e]	784	0.067	104	0.180	22	0.077	11	0.040	72	0.150
genes down-regulated at 4 dpi vs. *in vitro*[f]	1027	0.087	61	0.105	55	0.194	34	0.124	120	0.249
genes up-regulated at 13 dpi vs. 4 dpi[e]	1773	0.151	276	0.477	78	0.275	92	0.336	120	0.249
genes down-regulated at 13 dpi vs. 4 dpi[f]	798	0.068	48	0.083	61	0.215	15	0.055	113	0.235

Table 3. Continued

	Δkmt1/kmt6[h]			
	up-regulated		down-regulated	
	nb. in the genome	proportion	nb. in the genome	proportion
total number of genes	558		455	
H3K4me2[a]	72	**0.129**	147	**0.323**
H3K9me3[a]	8	0.014	10	0.022
H3K27me3[a]	248	0.444	69	0.152
H3K9/K27me3[a]	29	0.052	22	0.048
unknown[b]	420	0.753	157	**0.345**
CAZymes	7	0.013	10	0.022
putative effectors	65	0.116	62	0.136
genes < 2 Kb Tes[c]	138	0.247	125	0.275
orphan genes	166	0.297	50	0.110
genes expressed at 4 dpi vs axenic[d]	62	0.111	0	NA
genes expressed at 13 dpi vs axenic[d]	137	0.246	2	**0.004**
genes expressed at 13 dpi vs 4 dpi[d]	119	0.213	18	0.040
genes up-regulated at 4 dpi vs. *in vitro*[e]	94	0.168	25	0.055
genes down-regulated at 4 dpi vs. *in vitro*[f]	33	0.059	123	0.270
genes up-regulated at 13 dpi vs. 4 dpi[e]	229	0.410	117	0.257
genes down-regulated at 13 dpi vs. 4 dpi[f]	38	0.068	73	0.160

Table 3. Influence of *kmt1*, *kmt6* or *kmt1/kmt6* deletions on gene expression.

[a]Genes located in a H3K4me2, H3K9me3, H3K27me3 or H3K9me3, H3K27me3 *in vitro*;

[b]"unknown" genes are genes encoding predicted or hypothetical proteins;

[c]Genes located up to 2 kb upstream or downstream to a transposable element sequence;

[d]Genes specifically expressed at 4 or 13 days post infection (dpi) compared to axenic culture or 4 dpi when RPKM ≥ 2 at the time point and RPKM ≤ 2 during the axenic culture or at 4 dpi;

[e]Up-regulated genes are genes with Log2 Fold Change (RPKM) ≥ 1 and FDR ≤ 0.001 in a given condition compared to the other;

[g]Down-regulated genes are genes with Log2 Fold Change (RPKM) ≤ -1 and FDR ≤ 0.001 in a given condition compared to the other;

[h]Genes deregulated in *KMT1*, *KMT6* or *KMT1/KMT6* deletions background, Log2 Fold Change (RPKM) ≤ -1 or ≥ 1 and FDR ≤ 0.001.

Bold: the given domain contains significantly less genes of the given category compared to the rest of the genome; grey: the given domain is enriched for the category of genes compared to the rest of the genome.

Table 4. Expression of selected genes associated with heterochromatin *in vitro*, in a *kmt1*, kmt*6* and kmt*1/kmt6* deletion background.

							in planta expression[d]	relative expression vs. WT[e]		
ID	orphan[a]	TE[b]	SP[a]	H3K4me2[c]	H3K9me3[c]	H3K27me3[c]	up 13 vs 4 dpi	*Δkmt1*	*Δkmt6*	*Δkmt1/kmt6*
Zt09_chr_2_00407	-	yes		-	yes		-	2	3	7
Zt09_chr_2_00483	yes	-	-	-	-	yes	-		3	2-8
Zt09_chr_3_00231	yes	yes	yes	-	-	yes	6	-	-	-
Zt09_chr_4_00279	-	yes	yes	-	yes		6	-	3-5	-
Zt09_chr_8_00723	yes	yes		-			3	2-5	200	20
Zt09_chr_9_00004	-	yes		-	yes	yes	3	6-16	65-90	~9
Zt09_chr_9_00005	-	yes	yes	-	yes	yes	8	-	40	~3
Zt09_chr_11_00525	-	yes		-	yes	yes	6	20-69	200-1000	140
Zt09_chr_13_00020	-	-	-	-	-	yes	10	1-4	28-36	6-9

[a]Genes located up to 2 kb upstream or downstream to a transposable element sequence;
[b]Genes located in a H3K4me2, H3K9me3, H3K27me3 or H3K9me3, H3K27me3 *in vitro*;
[c]Genes significantly up-regulated 13 days post-infection (dpi) compared to 4 dpi;
[d]Gene expression relative to the WT strain and to the GAPDH encoding gene.

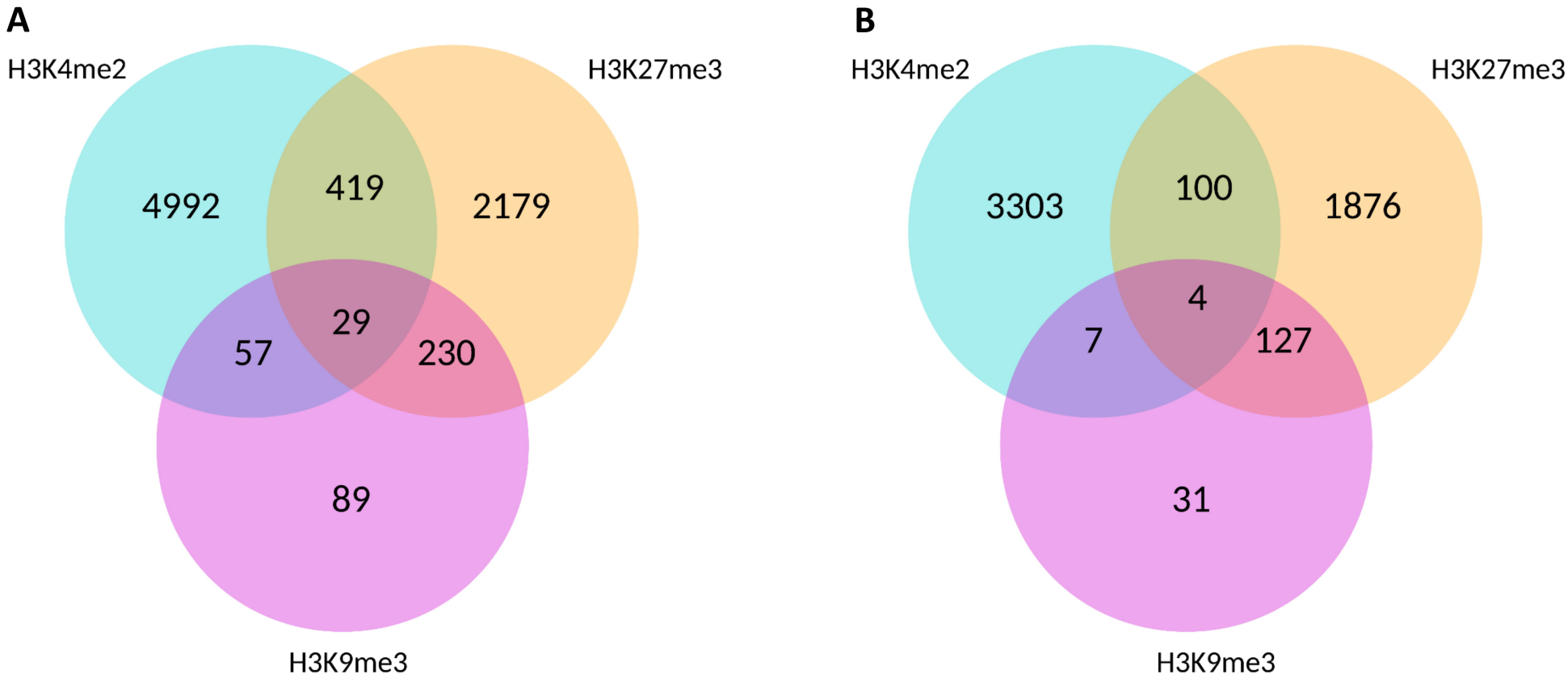

Figure 1. Euchromatic domains encompass more genes than heterochromatin domains *in vitro*. Venn diagrams showing genes associated with the different post-translational histone modifications assessed using ChIP-sequencing in axenic culture. A) Genes at least partially associated with any of the histone modification. B) Genes completely associated with any of the histone modifications.

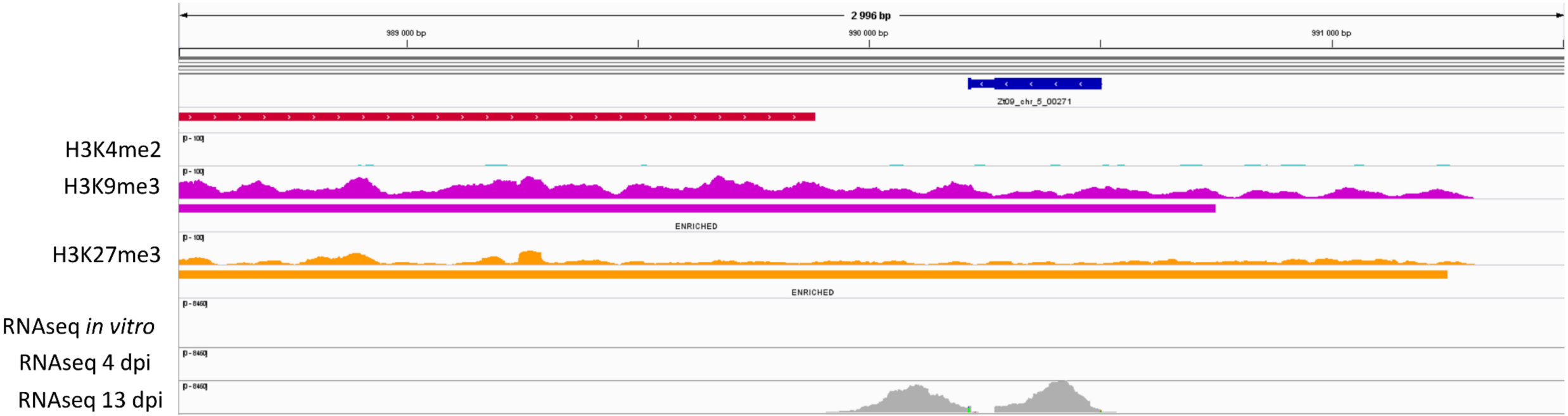

Figure 2. Heterochromatic domains are enriched with putative effector genes that are up-regulated during the switch towards necrotrophic growth on wheat. Example from a section of chromosome 5, harboring the putative effector gene ID Zt09_chr_5_00271. Regions enriched in different histone modifications were identified using ChIP-seq with antibodies against H3K4me2 (light blue), H3K9me3 (purple), H3K27me3 (orange) and compared to the location of genomic features (coding sequences, dark blue; transposable elements, red) and to reads obtained by RNA-seq in axenic culture, 4 days post-infection (dpi) and 13 dpi.

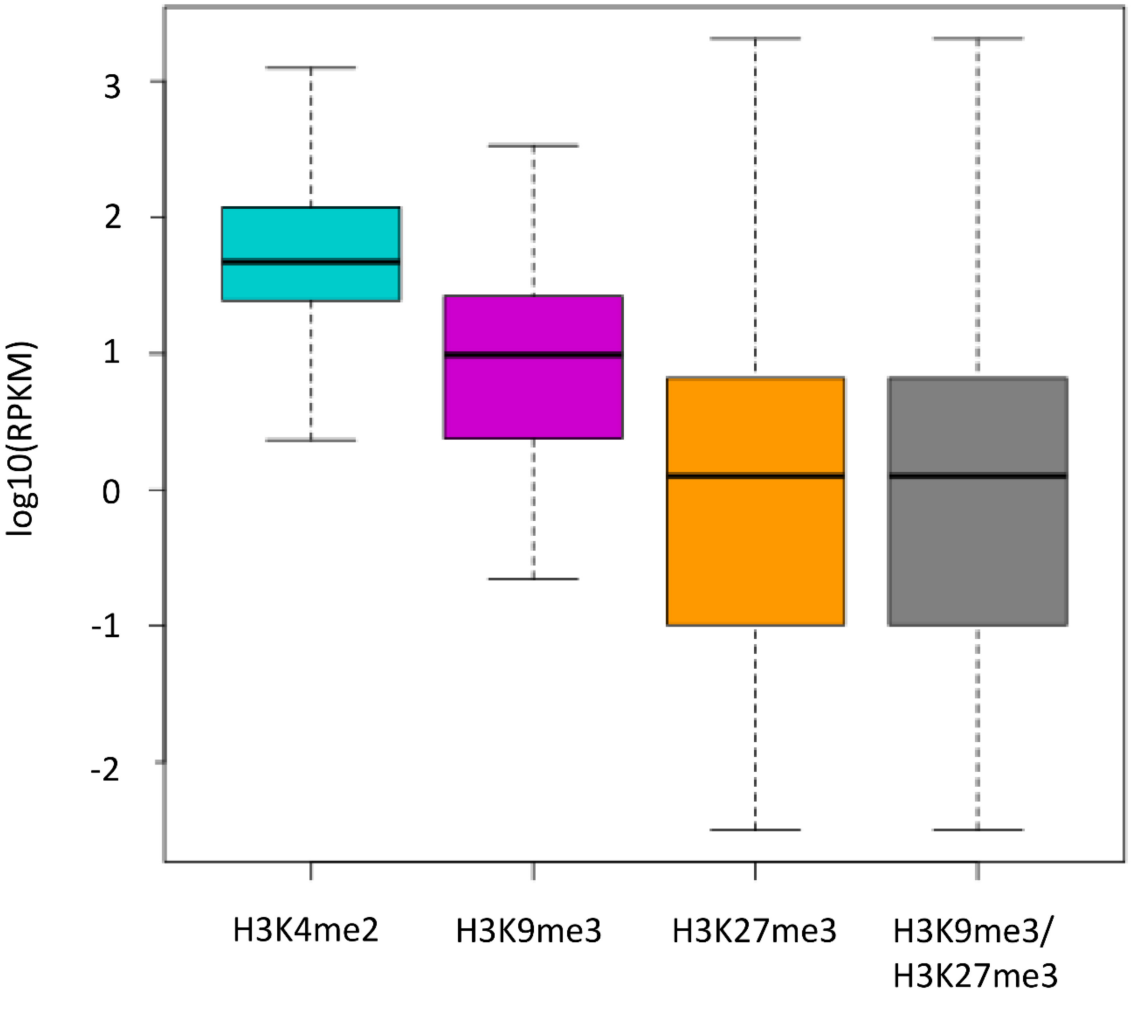

Figure 3. Genes associated with euchromatin are expressed while genes associated with heterochromatin are repressed. Expression assessed during axenic culture using RNA-sequencing. Boxplot of the $\log_{10}$(RPKM) of the genes totally associated with any of the histone modification.

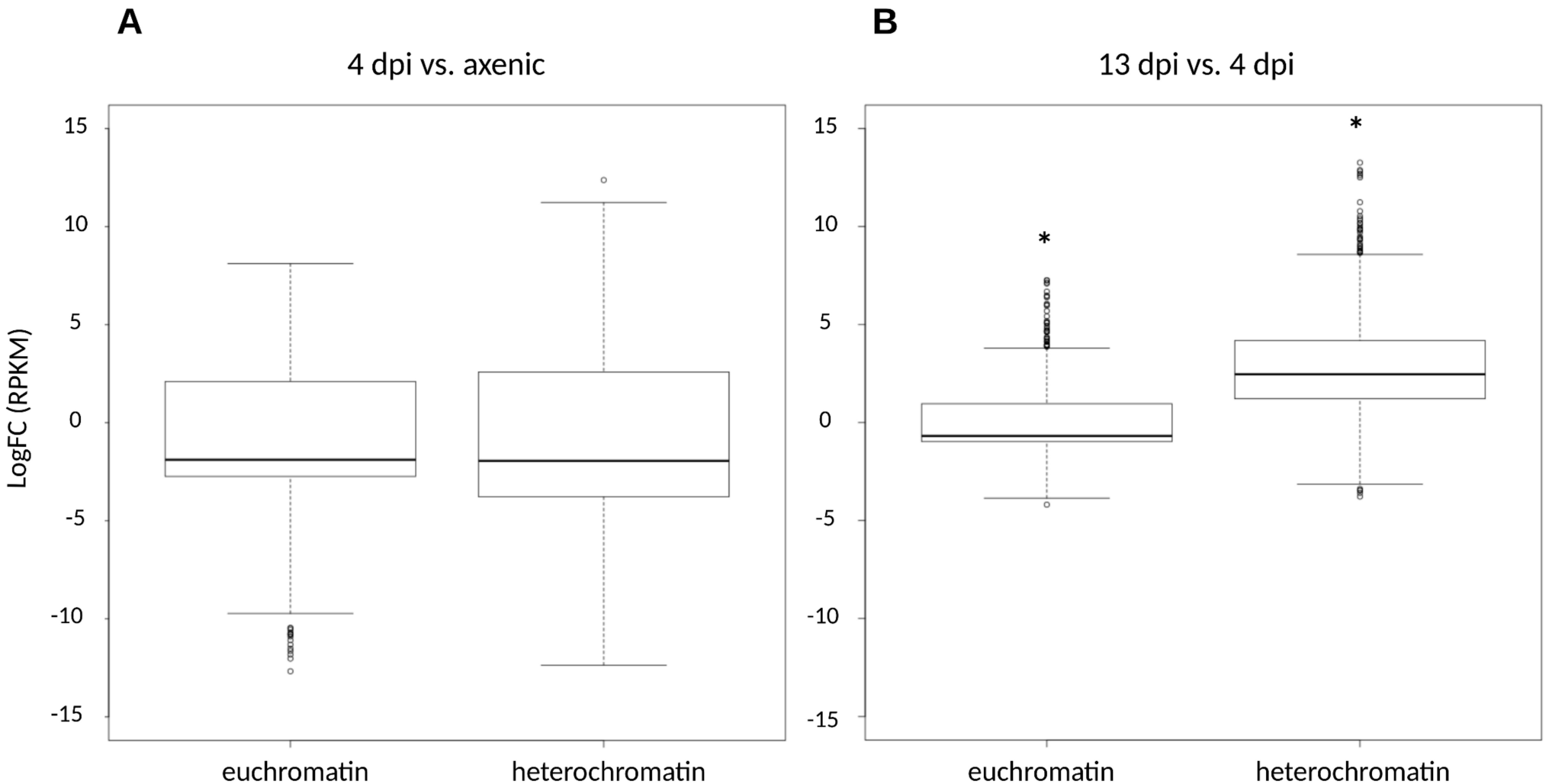

Figure 4. Genes associated with euchromatin and heterochromatin *in vitro* exibit different expression profiles *in planta*. Boxplot of the $\log_{10}$ Fold Change (RPKM) of the genes located in a euchromatic domain *in vitro* (i.e. H3K4me2) or a heterochromatic domain *in vitro* (i.e. H3K9me3, H3K27me3 or H3K9me3/H3K27me3). Expression assessed during axenic culture and at 4 and 13 days post infection (dpi) using RNA-sequencing; genes differentially expressed at 4 dpi vs. axenic culture (A) or 13 dpi vs. 4 dpi (B). *: Wilcoxon-test, $P < 2.2.10^{-16}$: comparison of heterochromatic-associated genes between 4 and 13 dpi.

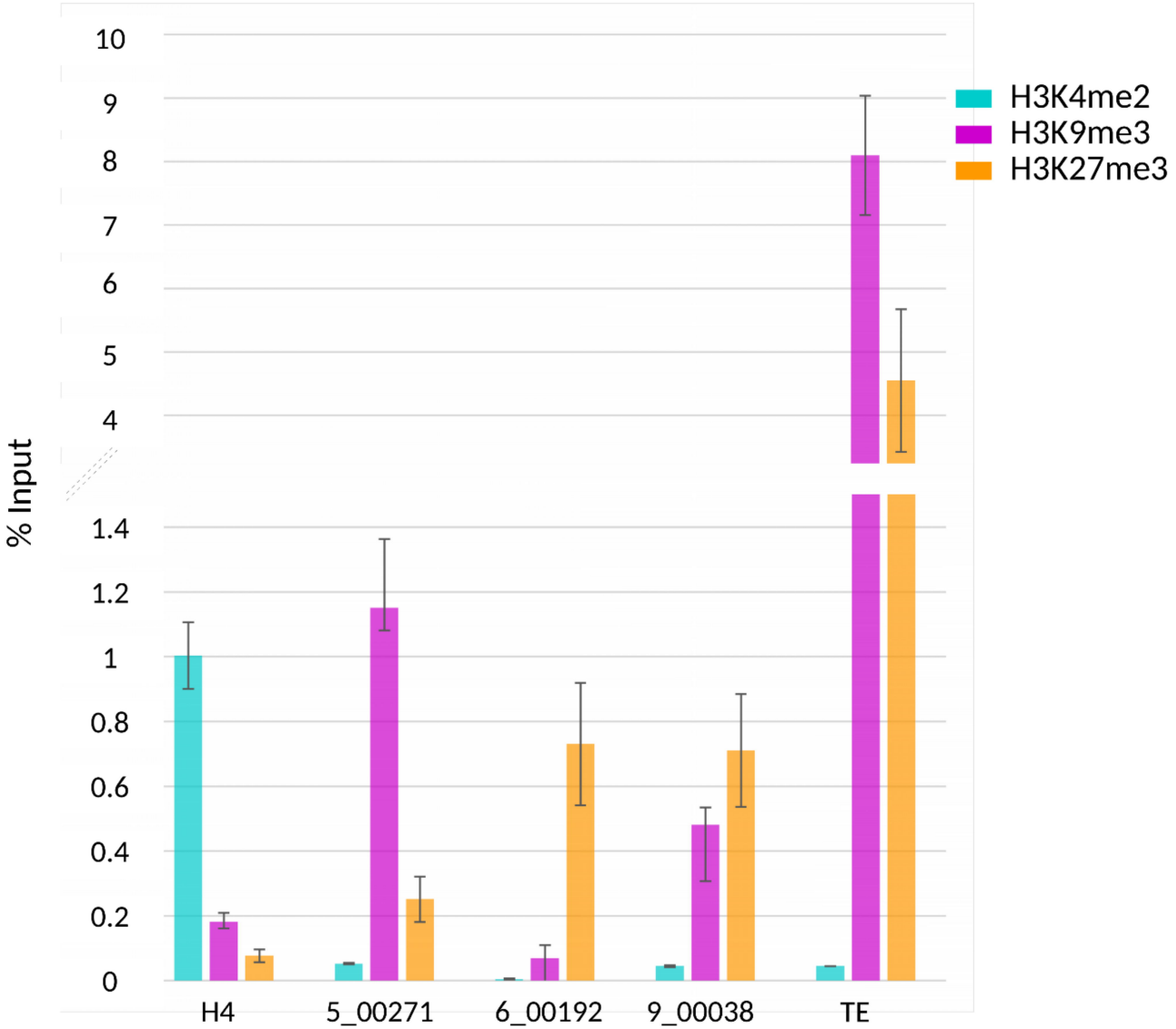

Figure 5. Putative effector genes are enriched in H3K9me3 and/or H3K27me3 *in vitro* while histone H4 is enriched in H3K4me2. Chromatin immunoprecipitation was performed during axenic culture to assess the levels of H3K4me2, H3K9me3 and H3K27me3 in the genomic sequence of four genes (H4, Histone H4: Zt09_chr_6_00256; 5_00271: Zt09_chr_5_00271; 6_00192: Zt09_chr_6_00192; 9_00038: Zt09_chr_9_00038) and a transposable element (DTH_element5_ZTIPO323).

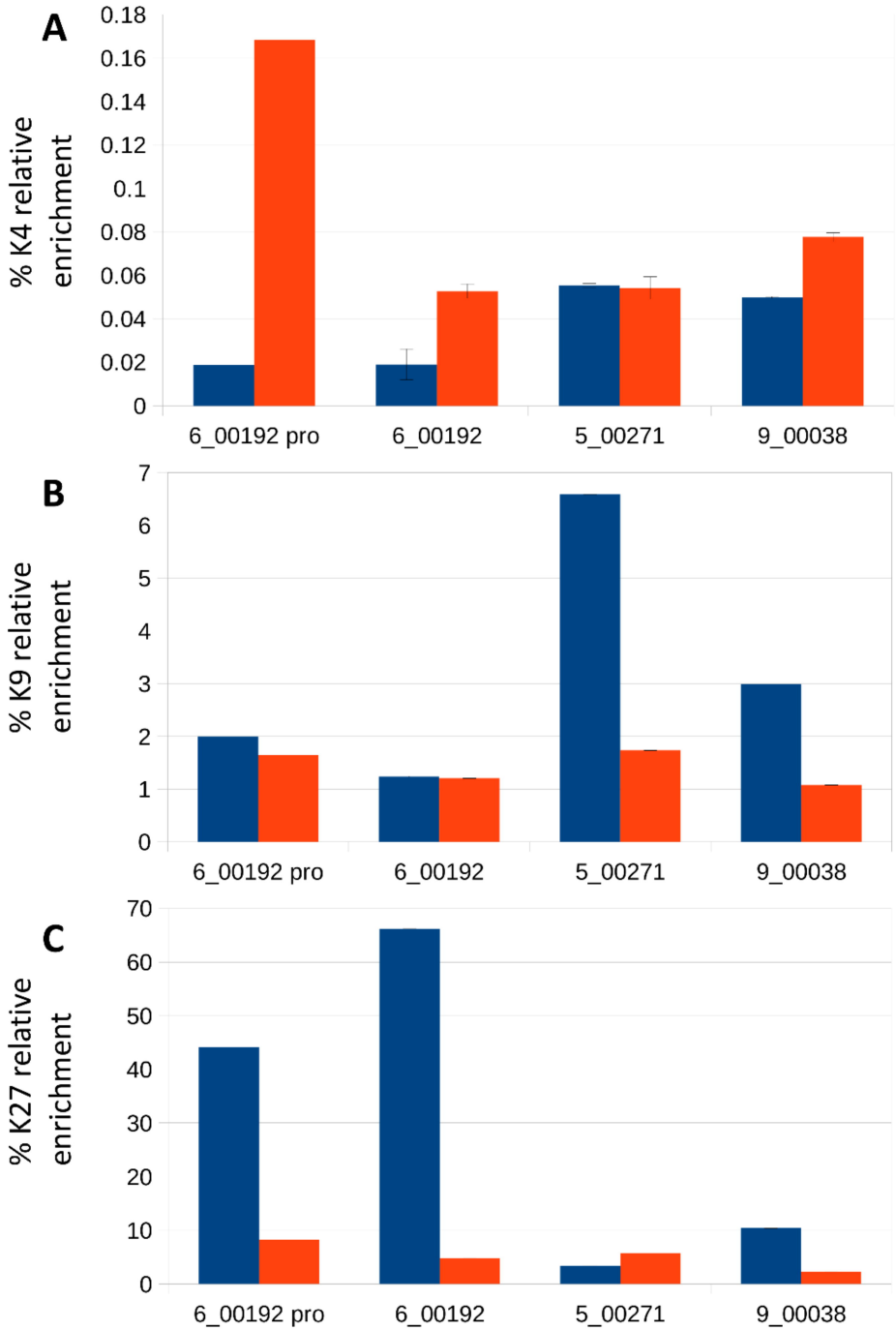

Figure 6. The up-regulation of three effector genes *in planta* is associated with a change of their histone modifications patterns. ChIP was performed at 13 days post infection of wheat leaves by *Zymoseptoria tritici* and relative enrichment of (A) H3K4me2, (B) H3K9me3 and (C) H3K27me3 was assessed using qPCR and compared during the axenic culture and at 13 dpi. 5_00271: Zt09_chr_5_00271; 6_00192: Zt09_chr_6_00192; 6_00192 pro: Zt09_chr_6_00192, promoter; 9_00038: Zt09_chr_9_00038; K4, K9 and K27: H3K4me2, H3K9me3 and H3K27me3 respectively. Blue: axenic culture; red: 13 dpi.